Reactivity of Low-valent Iridium Thiolate Complexes

A thesis submitted to McGill University in partial fulfillment of the requirements of the degree

of

Master of Science

by

Mirna Paul

Department of Chemistry, Faculty of Science

McGill University

Montreal, Quebec, Canada



© 2014, Mirna Paul. All rights reserved.

ABSTRACT

A series of six-coordinate iridium thiol complexes, $HIr(SR)(X)L_2$ where $R = C_6H_5$, $C_6H_4CH_3$, or $C_6H_4NO_2$, X = Cl or I and $L = P(C_6H_5)_3$ or $(C_6H_5)_2PC_2H_4P(C_6H_5)_2$, have been synthesized by oxidative addition of four-coordinate precursors. Another series of metal complexes containing sulfur-rich ligands with the formula, $M(S_xCC_6H_4CH_3)$ or $M(S_xCC_6H_5)$ where M = Zn, Ni or Co have been prepared as well. The infrared and nuclear magnetic resonance spectra of these complexes are discussed with regard to possible structures for the isomers these compounds tend to form under varying conditions. Some of these results help to confirm the large *trans* effect some of these ligands have within their respective complexes and are reconfirmed by the crystal structures obtained in these studies. The alpha effect of lone pair-bearing substituents was also explored with focus on the enhanced nucleophilicity of adjacent thiol groups. The results of these studies are further described in this thesis.

RESUMÉ

Une série de six-coordonnés composés de thiol iridium, HIr(SR)(X)L₂ où R = C₆H₅, C₆H₄CH₃, ou C₆H₄NO₂, X = Cl ou I, et L = P(C₆H₅)₃ ou (C₆H₅)₂PC₂H₄P(C₆H₅)₂, a été synthétisée par addition-oxydante, en commençant par les précurseurs de quatre-coordonnés. Une autre série de complexes métalliques contenant des ligands riches en soufre ayant la formule, M(S_xCC₆H₄CH₃) ou M(S_xCC₆H₅), où M = Zn, Ni ou Co, a été préparé aussi. Les spectres d'infrarouge (IR) et les spectres de résonance magnétique nucléaire (RMN) ont été analysés pour la détermination des structures des isomères de ces composés qui se sont formé dans des conditions variables. Les résultats obtenus ont permis de confirmer l'effet *trans* au niveau de certains ligands de ces complexes. Ceci a également été confirmé par l'analyse des structures cristallines obtenus de ces composés. Les résultats de ces études sont décrits en detail dans le présent mémoire.

PREFACE AND CONTRIBUTIONS OF AUTHORS

The work in this thesis was carried out solely by the author under the supervision of Dr. D.S. Bohle. Mirna Paul designed and performed the experiments, as well as analyzed the data while Dr. D.S. Bohle contributed all the computational calculations.

TABLE OF CONTENTS

Table of contents	1
1. Introduction: Thiolate Derivatives and Their Nucleophilicity in Metal Complexes	3
1.1. Chemistry of Sulfur and Thiol Functional Groups.	3
1.2. Illustrations of Nucleophilic Thiol Reactivity	6
1.3. The α-effect in Polar Ligands and Their Enhanced Reactivity	7
1.4. The α-effect in Metal-mediated Mechanisms.	8
1.5. Enzymatic Sulfur Transformations	11
1.6. Biomimetic Transition Metal Complexes	17
1.7. References	21
2. Synthesis of Six-coordinate Iridium ^(III) Thiolate Complexes	26
2.1. Introduction.	26
2.2. Experimental	26
2.2.1. Synthesis of HIrCl(SH)(CO)(PPh ₃) ₂	27
2.2.2. Synthesis of HIrClI(CO)(PPh ₃) ₂	27
2.2.3. Synthesis of HIrCl(SC ₆ H ₅)(CO)(PPh ₃) ₂	28
2.2.4. Synthesis of HIrCl(SC ₆ H ₄ CH ₃)(CO)(PPh ₃) ₂	28
2.3. Results and Discussion.	29
2.4. Isomers.	41
2.5. Reactivity of Complex I.	43
2.6. Conclusions	47
2.7. References	48
3. Activated Low-valent Ir ^(I) and Ir ^(III) Thiolate Complexes	51
3.1. Introduction.	51
3.2. Experimental	51

3.2.1. Synthesis of [IrH(SC ₆ H ₅)(dppe) ₂]Cl	52
3.2.2. Synthesis of [IrH(SC ₆ H ₄ NO ₂)(dppe) ₂]Cl	53
3.2.3. Synthesis of IrHCl(SC ₆ H ₅)(PPh ₃) ₂	53
3.2.4. Synthesis of IrHCl(SC ₆ H ₄ CH ₃)(PPh ₃) ₂	53
3.2.5. Synthesis of IrCl(SC ₂ H ₄)(PPh ₃) ₂	54
3.3. Results and Discussion.	54
3.4. Conclusions.	61
3.5. References	63
4. Compounds with Sulfur-rich Ligands	65
4.1. Introduction.	65
4.2. Experimental	66
4.2.1. Synthesis of Zn(S ₃ CC ₇ H ₇) ₂	67
4.2.2. Synthesis of Zn(S ₂ CC ₇ H ₇) ₂	67
4.2.3. Synthesis of Ni(S ₃ CC ₇ H ₇)(S ₂ CC ₇ H ₇)	68
4.2.4. Synthesis of CH ₂ (S(CS)C ₇ H ₇) ₂	68
4.3. Results and Discussion.	69
4.4. Preparation and Structural Analysis for CH ₂ (S(CS)C ₇ H ₇) ₂	74
4.5. Conclusions.	80
4.6. References	81
5. Conclusions and Future Work	84
6. Acknowledgments.	87
7. Appendix	89

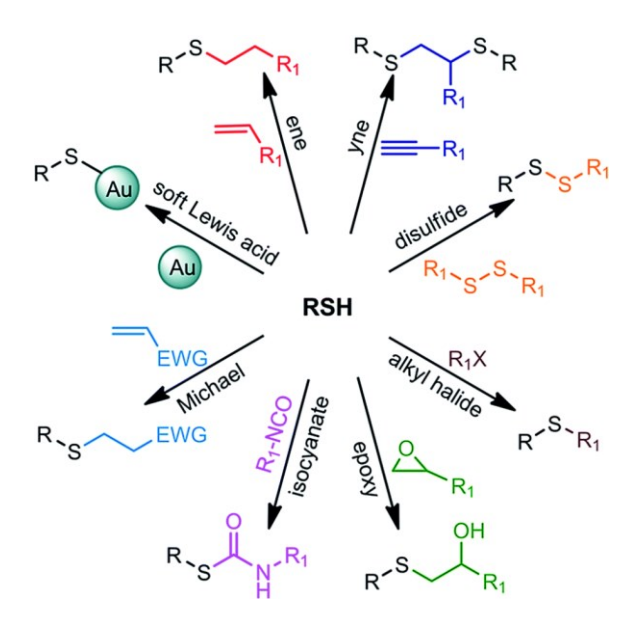
CHAPTER ONE

Thiolate Derivatives and Their Nucleophilicity in Metal Complexes

1.1 Chemistry of Sulfur and Thiol Functional Groups

In the past several years there has been an increased interest in the chemistry of sulfur derivatives in transition metal complexes due to their use in biological, synthetic and environmental applications. Many sulfur-containing compounds bear no fundamental difference between their corresponding oxygen analogues, though in a few cases they can be more reactive; i.e. thioesters versus esters, or the acidity of thiols versus alcohols.^{1,2}

Thiols can interconvert into copious functional groups including, but not limited to sulfides, sulfoxides, sulfones, sulfonic acids, thioacetals and thioacids. They may also react with a range of functional groups to form other reactive derivatives (Scheme 1). In many inorganic compounds sulfur-sulfur disulfide bridge linkages also form, yielding sulfur-rich ligands such as dithiocarboxylate and perthiocarboxylate groups.



Scheme 1. Various transformations of monothiols undertake with other functional groups.

Due their ability to undergo such numerous transformations, thiols are frequently used in synthetic methodologies in which the group is usually converted into the final product. Synthetic processes that require only a single thiol transformation are far rarer as in many cases this group is used in the preparation of new sulfur-containing derivatives and must therefore be regenerated through other subsequent steps (Figure 1).³

$$H_2O$$
 $Ar-SH$
 $E-Se-S-Ar$
 $E-SeO_2H$
 $Ar-SS-Ar$
 $E-SeO_1$
 $Ar-SS-Ar$
 $E-SeO_2$
 $Ar-SS-Ar$
 $E-SeO_1$
 $Ar-SS-Ar$
 $E-SeO_1$
 $E-SeO_2$
 $E-SeO_2$
 $E-SeO_1$
 $E-SeO_2$
 $E-SeO_1$
 $E-SeO_2$
 $E-SeO_2$
 $E-SeO_1$
 $E-SeO_2$
 $E-SeO_2$
 $E-SeO_1$
 $E-SeO_2$
 $E-SeO_2$
 $E-SeO_2$
 $E-SeO_3$

Figure 1. Catalytic cycle of semi-synthetic peroxidase selenosubtilisin, where E = selenosubtilisin, and ArSH = 5-thio-2-nitrobenzonic acid. The Ar-S-S-Ar disulfide group regenerates ArSH upon hydrolysis.

Thiols may also act as nucleophiles in two principal kinds of reactions, either by a substitution or addition to another bond. For example, 2-lithio-1,3-dithianes can be considered masked nucleophilic acylating reagents due to their participation in reactions with a myriad of electrophiles to yield substituted thianes (Figure 2).⁴ The carbonyl carbon of the original aldehyde thus transforms from a normally electrophilic site to a nucleophilic center due to the ability of the sulfur to stabilize carbanions in the position α to the sulfur atom, allowing for nucleophilic substitution by lithiation or an electrophile.⁵

Figure 2. Mechanisms for the synthesis of dithianes and its reactions with electrophiles, where R = H, alkyl or aryl groups.

In nucleophiles, where the thiolate anion, RS, is acting as the primary nucleophile, the acidity of the thiol proton is significant with $pK_a < 7$. It is possible to produce thiolate nucleophiles in non-aqueous solutions by other pathways such as the hydrolysis of thiourea derivatives but these types of substitution reactions are not limited to organic groups. 6 Several main group and transition metals coordinate sulfur as nucleophilic thiols/thiolates, which generally tend to exhibit stronger nucleophilic strength than alcohols/alkoxides. Not all thiolates show nucleophilic reactivity, however, as this property seems to be heavily influenced by steric effects. Pentachlorobenzenethiolate (C₆Cl₅SH), for instance, demonstrates little nucleophilicity as a ligand while RC_6H_4SH (R = H, methyl or tert-butyl) makes effective nucleophiles, where the rates of reactivity increase as R becomes less substituted. Pentaflurobenzenethiolate (C-₆F₅SH) in comparison is also much more reactive than its chlorine analogue, most likely due to the differences size-to-charge ratio of the halogens. C₆Cl₅SH has more delocalized charge on the thiolate anion, thus causing for it to be less nucleophilic. In bioinorganic systems, this negative charge, rather than be delocalized by an aromatic π -system, tends to help stabilize the high oxidation state changes of central metal ions, allowing them to engage in various redox reactions as well.

1.2 Illustrations of Nucleophilic Thiol Reactivity

The role of thiols in synthetic, biological and industrial applications has increased in recent years due to innovations in enhancing the nucleophilic reactivity of these compounds toward substitutions and formulation processes as well as several other uses. Nucleophilic thiols cover a broad range of versatile reactions, not limited to the phosphorylation of *S*-nucleophile by substitution,⁷ alkylation of sulfur in a metal Mo complex,⁸ the inhibition of reactive electrophilic metabolites through covalent binding⁹ as well as the catalytic activity of some hydrolytic enzymes.¹⁰ Reactive thiolates can also be found as the active nucleophile in certain coenzymes¹¹ and can contribute to the detoxification of enzymatic inhibitors via conjugation¹² along with the formation of thiosemicarbazones that display enhanced antiviral reactivity.¹³ Though usually aromatic, alkyl nucleophilic thiols have also been shown to participate in enantioselective conjugated addition to unsaturated aldehydes by multicomponent reactions.¹⁴ Nucleophilic thiolates can now even be detected by analytical fluorescence as new probes are formulated with disulfide bridges that undergo thiol-disulfide exchange reactions to indicate the presence of the nucleophile (Scheme 2).¹⁵

Scheme 2. Synthesis of fluorescent probe and mechanism of thiol-sensing based on FRET, where FITC = fluorescein isothiocyanate, and light emission is seen upon reaction of the probe with a thiol compound.

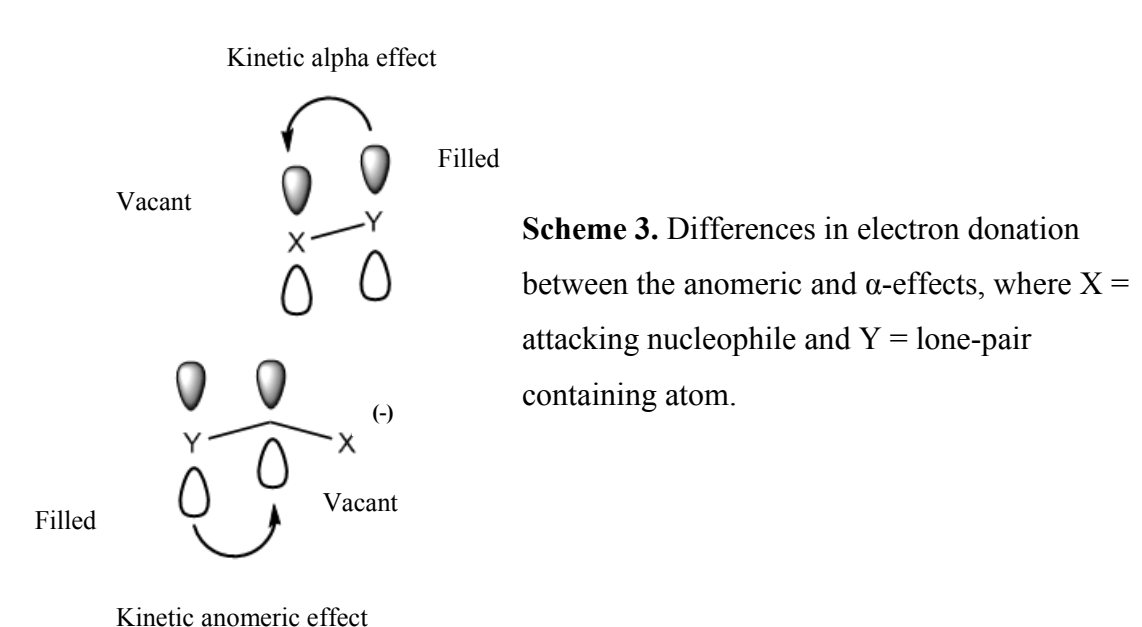
1.3 The α-effect in Polar Ligands and Their Enhanced Reactivity

There are several instances in literature of increased reactivity of nucleophiles when the atom adjacent to the attacking atom contains one or more unshared pairs of electrons. Some examples of such nucleophiles are hydrazine, hypochlorite, perhydroxide, acetone oximate, as well as many other compounds which react more readily than molecules without lone pairs on the atom adjacent to the nucleophilic center. There appears to be no single factor for this phenomena but rather a sum of several factors, not limited to the repulsion between adjacent pairs of electrons, the ground-state stabilization of the nucleophile, transition-state stabilization, solvent effects and thermodynamic product stability. ¹⁶

For example, perhydroxide (HOO⁻), one of the strongest nucleophiles, is about 10 to 10² more reactive in magnitude than hydroxide depending on the substrate and this difference can be attributed to a variety of causes, including hydrogen bonding by OOH⁻ in the transition state, the diminished solvation of the α-nucleophile compared to non-alpha nucleophiles and the stability of the nucleophilic addition products of perhydroxide as it makes a worse leaving group than hydroxide. This effect is also seen in *N*-nucleophiles such as hydrazine and *P*-nucleophiles like phosphonothiolate, and is usually limited to second and third row electronegative elements where electronic effects are more likely to occur. ^{17,18}

As the α -effect not only tends to increase the general reactivity of a nucleophile but also the rate of subsequent reactions it is considered a kinetic effect, one that is not restrained to organic substituents. ¹⁹ Enhanced nucleophilicity can also be observed in organometallic compounds with polar substituents, many of which will be discussed in the following section. It is important not to confuse the influence of the anomeric effect with the α -effect even though

these two often go hand-in-hand since they are both exerted by lone pairs interacting with the transition states of nucleophilic additions.¹⁹ Whereas the anomeric effect can be thought of as a transition-state stabilization by electron donation from a lone-pair containing atom through hyperconjugation, the α-effect can be considered as a ground-state stabilization through electron delocalization around the X-Y bond (Scheme 3). While both can contribute to the overall reactivity of nucleophiles, the latter is of particular interest as the causes behind this influence are still widely speculated.



1.4 The α-effect in Metal-mediated Mechanisms

Coordinated transition metal complexes are known for being able to catalyze a variety of reactions in several applications ranging from biology to industry due to their relatively high redox potentials. Not only are some of these able to selectively bind their respective substrates but also show elevated kinetic reactivity in various reactions such as metal ion-promoted nucleophilic substitution. This type of catalysis usually involves nucleophilic activation which can also partially be attributed to transition state stabilization wherein the reactivity of the metal-

coordinated nucleophile is enhanced by the presence of the *d*-orbital electrons within the metal.²⁰ Numerous transition metal participate in such catalytic reactions, particularly early transition metals though there has been a myriad of examples of later transition metals and lanthanides displaying excellent catalytic activity.

Studies with La^(III) and Zn^(II) complexes show that they are able to catalyze the methanolysis of phosphonates in order to solvolytically destroy them, where the phosphonates were between 10⁵-fold and 10⁸-fold more reactive toward the attack of the metal-bound nucleophilic group than compared to the corresponding free ligand alone.²¹ Co^(II) complexes have been found to promote the hydrolysis of phosphodiesters into diethyl phosphates and phenolates with a rate enhancement of 10⁴-fold under ambient temperatures and neutral pH compared to hydrolysis under standard conditions.²² A micelle-based Cu^(II) complex proved to be an exceptional calayst for the hydrolysis a phosphate triester-containg nerve agent, *O*-pinacolyl methylfluorophosphonate, having a10⁵-fold rate enhancenement compared to the uncatalyzed reaction under the same conditions (Figure 3).²³

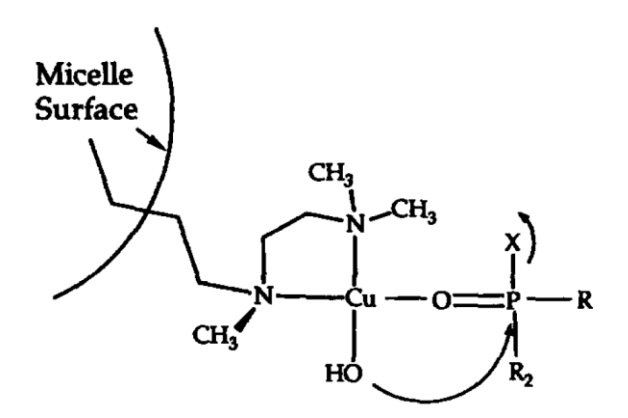


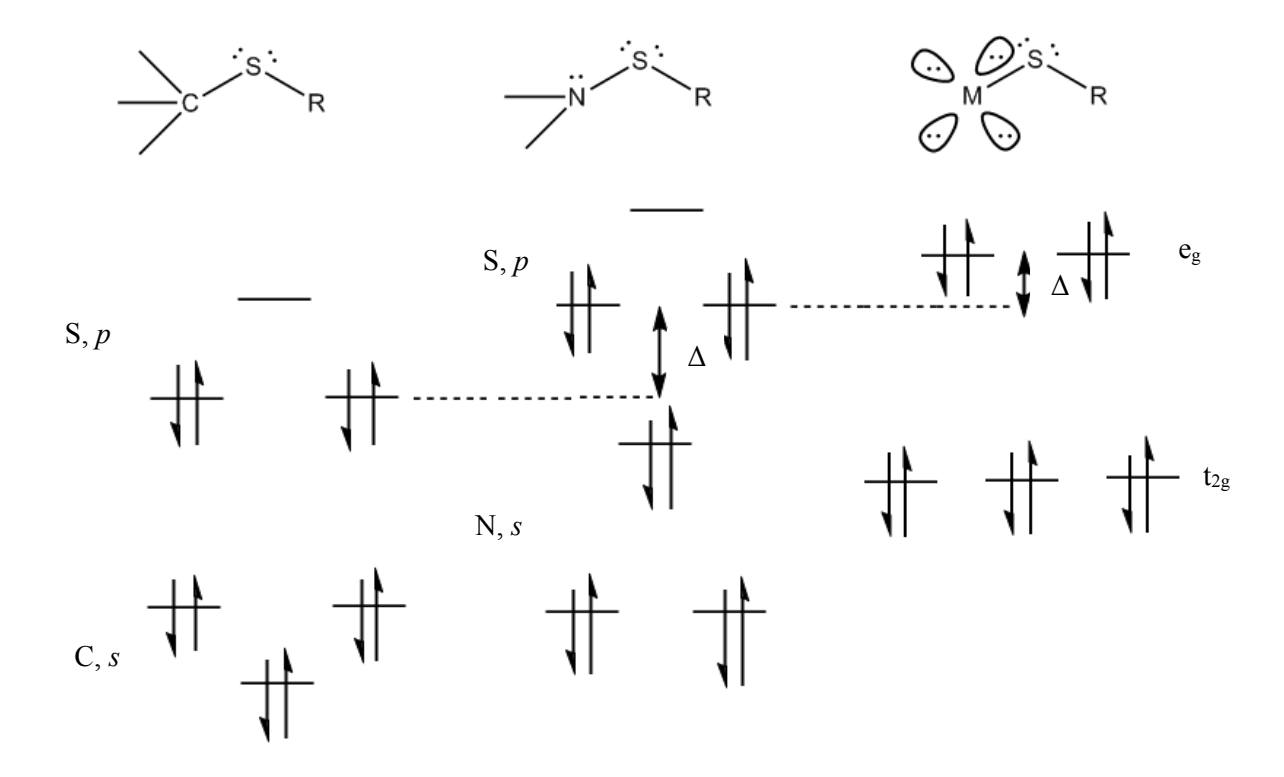
Figure 3. Scheme for the nucleophilic attack of a phosphate triester by a micelle-bound copper complex, where X = aryloxide or F, and R = alkyl and $R_2 = \text{alkoxide groups}$.

Another similar copper-based complex also catalyzes the same reaction despite macroligands that result in steric stacking effects (Figure 4).²⁴

Figure 4. Schematic structure of the binary complex formed upon coordination of a phosphate ester by a transition metal compound where $M = Cu^{2+}$ and $R = NO_2$.

This nucleophilic activation of respective ligands by the metal they are bound to is similar to the α -effect observed in organic polar substituents. Whereas the α -effect on the adjacent atom becomes more important as the *s*-character of the bonding orbitals increases, upon coordination to a transition metal with *d*-orbitals, this influence becomes even more evident. As a ground state stabilizing effect, this assumes that the alpha lone-pair and nucleophilic electron pair destabilize each other by electronic repulsion, thus raising the ground state and making the nucleophile more reactive (Scheme 4).

While the polarizability of the nucleophile does play a role, the investigation of this phenomenon is one of the major considerations on which this study was based with respect to the increased nucleophilic reactivity of metal bound-thiolates. Not only does being bound to a metal tend to make these thiolates more structurally stable, but this increase in reactivity also leads to an expansion in the scope of reactions these sulfur groups may be able to undertake.



Scheme 4. MO diagram for the influence of the α -effect in sulfur-containing compounds, where Δ is the increased energy of the ground state of the nucleophile with respect to the adjacent molecule.

1.5 Enzymatic Sulfur Transformations

The area of transitional metal sulfur species in bioinorganic chemistry covers a variety of different metals, including everything from enzymatic mononuclear centers to the heteropolynuclear active sites of metalloproteins. Typically, these transition metals are coordinated by sulfur in the form of either an inorganic donor group or an organic sulfur ligand, which often plays a key role in redox processes, catalysis or even substrate binding. The role of sulfur, especially in terms of biological relevance, is therefore quite ubiquitous. Sulfur coordination is necessary in the active centers of several enzymes including nitrogenase,

hydrogenase and cytochrome oxidase, and can also contribute an important structural role such as that found in zinc fingers. Considering that divalent zinc has no redox activity its function in catalytic processes usually involves polarizing effects or acid-base reactions, but other more electronically capable transition metals are able to participate in high-potential redox reactions.

One in particular, nitrous oxide reductase (N_2OR), has the unique ability to reduce nitrous oxide to elemental nitrogen (Figure 5). The mechanism for this reaction is still largely unknown, but it has been proposed that there is a two electron outer sphere reduction of N_2O by the active site's mixed-valence cuprous/cupric coupling, possibly similar to those also found in the active site of plastocyanins.^{25,26}

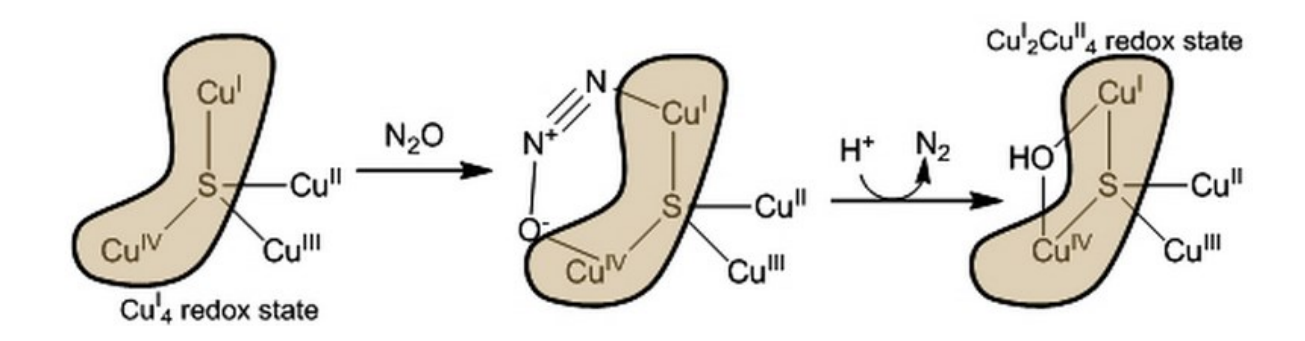


Figure 5: Scheme of the reduction mechanism of N₂O reductase for site Cu_A.

The problem with this proposed mechanism is the assumption that $Cu^{(I)}$ can develop enough redox potential to reduce N_2O , which does not appear to be the case given their relative standard potentials.

$$E^{0}/V$$
 $\log K$ $Cu^{2+} + e^{-} \rightleftharpoons Cu^{+}$ 0.16 2.7 $N_{2}O_{(g)} + 2H^{+} = 2e^{-} \rightleftharpoons N_{2(g)} + H_{2}O$ 1.77 59.7

Cu⁽¹⁾ does not have the oxidative potential to reduce N₂O as this molecule is largely inert compared to all other nitroxo compounds, indicating that there must be more to this mechanism than simply outer sphere electron transfer at work. It is possible to say that the mechanism for this reaction would have to rely on N₂O being bound by an electrophile. Given copper's oxidation states, however, it is likely that the metal is not involved in substrate binding as proposed by Figure 5.

Many metalloproteins owe their versatility to the prosthetic group ligands that bind their respective ions in the proteins, aiding to stabilize the charged metallic centers. For example, every copper ion in the active site of N₂OR is bound by two histidine residues (not shown in Figure 5) except for Cu^{IV}, which is only bound to one histidine residue in order to allow nitrous oxide to enter the enzymes binding site similar to how the heme group of cytochrome P450 coordinates a cysteine thiolate ligand in the position *trans* to the enzyme's O₂ activation site.

Such multi-metal copper-sulfur clusters are not unusual and often make up many of the enzymes found in both aerobic and anaerobic environments. Iron is another transition metal that also commonly forms such sulfur clusters, some ranging from simple like the metal centers for rubredoxins to complex, such as those found in aconitase (Figure 6). Again, these kinds of active sites undergo electron transfer between ferrous/ferric oxidation states, further facilitating redox reactions while maintaining high reactive turnover.

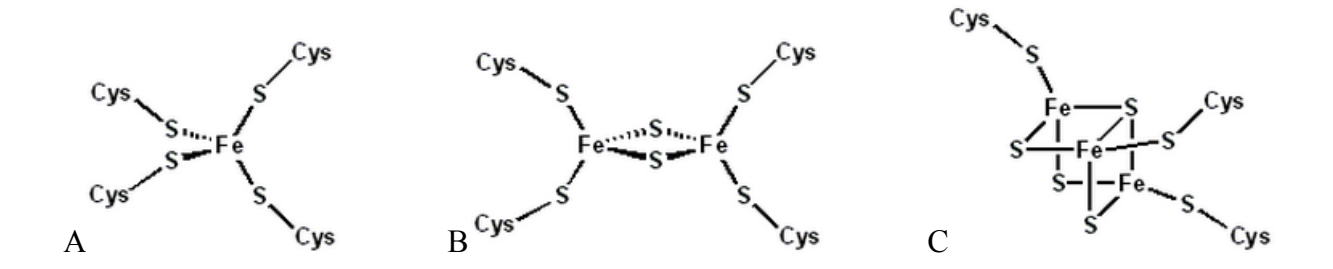


Figure 6. Enzymatic Fe-S clusters. A. Tetrahedral FeS₄ active site of rubredoxins. B. Dinuclear Fe₂S₂ center of ferrodoxins. C. Trinuclear Fe₃S₄ site of aconitase.

Other high oxidation state transition metals such as vanadium use sulfur coordination in the activation site of their enzymes and all molybdenum and tungsten proteins coordinate sulfur in their respective cofactors. ²⁷ Sulfite oxidase, for one, contains a molybdopterin cofactor at the center of its activation site that is bound by a cysteine residue and the dithiolene group of molybdopterin. The cofactor also supports a molybdenum^(VI) ion, which can bind sulfite and is able to oxidize the molecule through a series of electron transfer reactions to sulfate, thus undergoing an oxidation state change to molybdenum^(IV) (Figure 7). Although these are the most stable oxidation states for this element, the electron configuration of molybdenum allows it to be found in a variety of forms thus varying the functions of its different enzymes so greatly that it is considered a required element for all higher eukaryotic life forms except for some bacteria.

Figure 7. Transformation of sulfite into sulfate by mitochondrial sulfite oxidase.

In comparison, heteropolynuclear active sites might seem more uncommon, but they also tend to engage in very significant roles in biology. The thiolate-bound nickel sites of hydrogenase enzymes not only activate molecular hydrogen in order to oxidize it but are also capable of acting as ligands for other metals such as iron as they coordinate the cations through their sulfur atoms. Another important mixed-metal enzyme system is nitrogenase which contains an iron-molybdenum cofactor (FeMoco) that plays a considerable part in the activation of N₂ (Figure 8). The core structure has an overall octanuclear site consisting of two partial thiocubane structures which form a trigonal prism in the center of FeMoco with at least six of the central cations being of low-coordination number, allowing for binding of dinitrogen.²⁵ A recent study has also shown that this structure undergoes reversible loss of a sulfide ion in order to allow coordination of N₂.²⁸

Figure 8. FeMoco MoFe₇S₈ cofactor of nitrogenase.

Transition metal sulfur complexes have also seen increased use in commercial industries as they gain utility in effective catalytic systems. Of particular interest are those that promote the reduction of unsaturated molecules through hydrogenation of aromatic rings or perform in the removal of nitrogen, oxygen, sulfur or other metals from crude oil through processes known as hydrodenitrogenation, hydrodeoxygenation, hydrodesulfurization and hydrodemetallation, respectively. ²⁹⁻³¹

While significant efforts have been made in industry to mass produce these types of catalysts, special attention must be paid to the redox reactions these compounds engage in, which range from metal-based to ligand-based. Due to the reactivity of transition metal centers in various d-electron configurations, many systems with sulfur ligation exhibit substantial metal-based redox activity. Typically, these centers undergo a change in the coordination sphere of the metal or often involve an atom-transfer process, including dithiolene enzymes ranging from the dimethyl sulfoxide reductase family to the formate dehydrogenase family. Considering that sulfur-donor ligands have π -donor abilities it could be that the thiolate groups help facilitate these types of metallic redox reactions.

Non-transition metal sulfur derivatives on their own are also renowned for their redox capabilities, being found in both organic to inorganic molecules that range in oxidation states

from (-2) in ferrous sulfide to (+6) in ferrous sulfate. Those contained in metalloproteins are able to interconvert between these oxidation states fairly rapidly through redox processes, with some extensive enough to reduce every sulfur within the active site while leaving the metal oxidation states unchanged. There are several examples of the redox ability of sulfur ligands with transition metal complexes, both natural and synthetic, and it seems sulfur-donor ligand design contributes a large role in the reactivity, geometry and affinity of these metal cations.

1.6 Biomimetic Transition Metal Complexes

Given the diversity of the reactions that transition metal sulfur complexes found in nature can facilitate, it is not surprising that great effort has been made to synthesize similar imitative molecules. Biomimetic chemistry has become a larger part of both biology and industrial applications as the redox activity and general reactive nature of sulfur, combined with the high coordination ability of transition metals, leads to versatile chemistry that has heavily influenced these fields. Supplementing the synthesis of numerous new metal coordination and cluster compounds has offered complexes that give insight into structural, electronic-structural, and reactivity properties analogous to solid-state and protein structures. Many of these compounds are not only electronically noteworthy but also exhibit high reactivity such as that shown in Figure 9.³²

Figure 9. Proposed catalytic cycle for the production of H₂ from a molybdenum-oxo complex.

Similar to the active site of DMSO reductase, the molybdenum center is coordinated by at least five ligands with a resting oxidation state of (+4). The mechanism for this reaction involves a five-step process where the central ion goes through every oxidation state between Mo^(II) and Mo^(IV) in single electron transfers before finally reducing water to hydrogen gas. Though this model complex is coordinated by only pyridine derivatives, similar reactions have been generated using molybdenum-sulfur nanoparticles to catalyze the production of hydrogen gas from water by a ligand-centered proton reduction, ³³⁻³⁵ and all molybdenum centers in enzymes are coordinated by at least one dithiolene ligand.

Figure 10. Catalytic addition of sulfur to H₂ by a tungsten-oxo complex.

Related dithiolene ligands have also been used to model tungsten-oxo complexes such as the one in Figure 10, which is able to oxidize molecular hydrogen to hydrogen sulfide after abstracting two electrons from the protons.³⁶ Though mononuclear complexes are more extensively characterized in these types of reactions, several polynuclear transition metal clusters have been also been synthesized, from mixed-metal iron-iridium and iron-rhodium clusters³⁷ to a homonuclear tricopper-disulfido cluster that is able to reduce nitrous oxide to dinitrogen via outer sphere electron transfer reactions similar to those seen in the active site of N₂OR.³⁸

The diversity of these sulfur-transition metal transformations has established a basis for the reactions that have been further researched by this study. In our work, we are interested in generating potent metal bound nucleophiles. This series of experiments focuses on iridium^(III) complexes in particular due to the relative stability that the compounds display while still retaining their high reactivity. Noble metal sulfides such as those of ruthenium, rhodium and iridium are the most reactive binary metal-sulfide systems.³⁹⁻⁴¹ Sulfur-containing iridium and disulfide bond osmium complexes have already been found to be able to participate in in molecular hydrogen activation and the reduction of electrophiles.^{42,43} Further experimental work is needed to understand the underlying electronic causes for this observed periodic trend, but many iridium complexes can interchangeably undergo a number of oxidative additions.⁴⁴

Herein, the oxidative addition of thiols to four-coordinate iridium compounds react by a *cis* or *trans* mechanism to give complexes that contain versatile, substitutable hydrido and thiolato ligands. ⁴⁵ The stereochemistry of these transition metal substituted thiols, L_nMSR, has been determined via crystallography as well as by spectroscopic methods in order to establish exactly how the orientation of their ligands affect the complexes' reactivity. The chemical properties of these ligands were also examined in order to explore their catalytic potential. It is the goal of this study to investigate the receptiveness of the mercaptan group toward electrophilic substitution in hopes of eventually facilitating its subsequent use in biomimetic complex systems.

1.7 References

- 1. Patai, S.; Rappoport, Z. *The Chemistry of Sulphur-containing Functional Groups*. John Wiley & Sons: New York, **1993**.
- 2. Patai, S. The Chemistry of the Thiol Group, Part 1. John Wiley & Sons: New York, 1974.
- 3. van de Velde, F.; van Rantwijk, F.; Sheldon, R.A. Improving the catalytic performance of peroxidases in organic synthesis. *Trends in Biotech.*, **2001**, *19*(2), 73.
- 4. Corey, E.J.; Seebach, D. Carbanions of 1,3-dithianes. Reagents for C-C bond formation by nucleophilic displacement and carbonyl addition. *Angew. Chem.*, **1965**, *4*(*12*), 1075.; Corey, E.J.; Seebach, D. Synthesis of 1,η-dicarbonyl derivatives using carbanions from 1,3-dithianes. *Ange. Chem.*, **1965**, *4*(*12*), 1077.
- 5. Seebach, D. Nucleophilic acylation with 2-lithium-1,3-dithianes and 2-lithium-1,3,5-trithianes. *Synth.* **1969,** *1*(*1*), 17.
- 6. Patai, S. The Chemistry of the Thiol Group, Part 2. John Wiley & Sons: New York, 1974.
- 7. Panmand, D.S.; Tiwari, A.D.; Panda, S.S.; Monbaliu, J.M.; Beagle, L.K.; Asiri, A.M.; Stevens, C.V.; Steel, P.J.; Hall, C.D.; Katritzky, A.R. New benzotriazole-based reagents for the phosphonylation of various N-, O-, and S-nucleophules. *Tetrahed. Lett.*, **2014**, *55*, 5898.
- 8. Alonso, M.; Alvarez, M.A.; Garcia, M.E.; Gabriel-Vivo, D.; Ruiz, M.A. Nucleophilic behavior of dioxo- and dithiooxophosphorane complexes. *Dalton Trans.*, **2014**, *34*, 16074.
- 9. Hanafy, M.S.M.; Bogan, J.A. Pharmacological modulation of the pneumotoxocity of 3-methyllindole. *Biochem. Pharm.*, **1982**, *31(9)*, 1765.

- 10. Zhang, Z.; Wu, L. The single sulfur to oxygen substitution in the active site of nucleophile Yersinia protein-tyrosine phosphatase leads to substantial structural and functional perturbations. *Biochem.*, **1997**, *36*, 1362.
- 11. Allen, J.R.; Clark, D.D.; Krum J.G.; Ensign, S.A. A role for coenzyme M (2-mercaptoethanesulfonic acid) in a bacterial pathway of aliphatic epoxide carboxylation. *Biochem.*, **1999**, *96*, 8432.
- 12. Bunting, K.D.; Townsend, A.J. Dependence of aldehyde dehydrogenase-mediated oxazaphosphorine resistance on soluble thiols. *Biochem. Pharm.*, **1998**, *56*, 31.
- 13. Marigo, M.; Schulte, T.; Franzen, J.; Jorgensen, K.A. Asymmetric multicomponent domino reactions and highly enantioselective conjugated addition of thiols to α,β-unsaturated aldehydes. *J. Am. Chem. Soc.*, **2005**, *127*, 15710.
- 14. Moreno-Rodriguez, A.; Salazar-Schettino, P.M.; Bautista, J.L.; Hernandez-Luis, F.; Torrens, H. Guevara-Gomez, Y.; Pina-Canseco, S.; Torres, M.B.; Cabrera-Bravo, M.; Martinez, C.M.; Perez-Campos, E. In vitro antiparasitic activity of new thiosemicarbazones in strains of trypanosome cruzi. *Eur. J. Med. Chem.*, **2014**, *87*, 23.
- 15. Zheng, L.; Li, Y.; Yu, X.; Xu, J.; Chen, H. A sensitive and selective detection method for thiol compounds usuing novel fluorescence probe. *Anal. Chim. Acta*, **2014**, *850*, 71.
- 16. Fina, N.J.; Edwards, J.O. The alpha effect. A review. *Inter. J. Chem. Kin.*, 1973, 5, 1.
- 17. Fountain, K.R.; Felkerson, C.J.; Driskell, J.D.; Lamp, B.D. The α-effect in methyl transfers from S-methyldibenzothiophenium fluoroborate to substituted N-methylbenzohydroxamates. *J. Org. Chem.*, **2003**, *68(5)*, 1810.

- 18. Morales-Rojas, H.; Moss, R.A. Phosphorolytic reactivity of o-iodosylcarboxylates and related nucleophiles. *Chem. Rev.*, **2002**, *102*, 2497.
- 19. Cleplak, A.S. Stereochemistry of nucleophilic addition to cyclohexanone. The importance of two-electron stabilizing interactions. *J. Am. Chem. Soc.*, **1981**, *103*(*15*), 4540.
- 20. Yatsimirsky, A.K. Metal ion catalysis in acyl and phosphoryl transfer: Transition states as lignads. *Coord. Chem. Rev.*, **2005**, *249*, 1997.
- 21. Lewis, R.E.; Neverov, A.A.; Brown, R.S. Mechanistic studies of La³⁺ and Zn²⁺-catalyzed methanolysis of O-ethyl O-aryl methylphosphonate esters. *Org. Biomol. Chem.*, **2005**, *3*, 4082.
- 22. Hay, R.W.; Govan, N. The $[CoN_4(OH)(OH_2)]^{2+}$ (N₄ = trpn, cyclen and tren) promoted hydrolysis of the phosphoester 2.4-dinitrophenyl diethyl phosphate. *Trans. Met. Chem.*, **1998**, 23, 721.
- 23. Hay, R.W.; Govan, N.; Parchment, K.E. A metallomicelle catalyzed hydrolysis of a phosphate trimester, a phosphonate diester and O-isopropyl methylfluorophosphonate. *Inorg. Chem. Comm.*, **1998**, *1*, 228.
- 24. Negi, S.; Schneider, H. Metal coordination and stacking effects in supramolecular catalysis. Effects of structural variations of copper complexes for the hydrolysis of phosphate esters.
- 25. Butler, C.S.; Richardson, D.J. The emerging molecular structure of the nitrogen cycle: an introduction to the proceedings of the 10th annual N-cycle meeting. *Biochem. Soc. Trans.*, **2005**, *33*, 113.
- 26. Dell'Acqua, S.; Pauleta, S.R. The tetranuclear copper active site of nitrous oxide reductase. *J. Biol. Inorg. Chem.*, **2011**, *16*, 183.

- 27. Stiefel, E.I.; Matsumoto, K. Transition Metal Sulfur Chemistry. ACS: Honolulu, 1996.
- 28. Spatzal, T.; Perez, K.A.; Einsle, O.; Howard, J.B.; Rees, D.C. Ligand binding to the FeMO-cofactor: Structures of CO-bound and reactivated nitrogenase. *Science*, **2014**, *345*(*6204*), 1620.
- 29. Ho, T.C. Hydrodenitrogenation catalysis. Catal. Rev. –Sci. Eng., 1988, 30(1), 117.
- 30. Delmon, B. Selectivity in HDS, HDN, HDO and hydrocracking contribution of remote control and other new concepts *Bull. Soc. Chim. Belg.*, **1995**, *104*, 173.
- 31. Topsoe, H.; Clausen, B.S.; Massoth, F.E. *Hydrotreating Catalysis*. Springer Verlag: Berlin, **1996**.
- 32. Karunadasa, H.I.; Chang, C.J.; Long, J.R. A molecular molybdenum-oxo catalyst for generating H₂ from water. *Nature*, **2010**, *464*, 1329.
- 33. Hinnemann, B. Moses, P.G.; Bonde, J.; Jorgensen, K.P.; Nielsen, J.H.; Horch, S.; Chorkendorff, I.; Norskov, J.K Biomimetic hydrogen evolution: MOS₂ nanoparticles as catalyst for hydrogen evolution. *J. Am. Chem. Soc.*, **2005**, *127*, 5308.
- 34. Jaramillo, T.F.; Jorgensen, K.P.; Bonde, J.; Nielsen, J.H.; Horch, S. Identification of active edge sites for electrochemical H₂ evolution from MoS₂ nanocatalysts. *Science*, **2007**, *317*, 100.
- 35. Hou, Y.; Abrams, B.L.; Vesborg, P.C.K.; Bjorketun, M.E.; Herbst, K.; Bech, L.; Setti, A.M.; Damsgaard, C.D.; Pedersen, T.; Hansen, O.; Rossmessi, J.; Dahl, S.; Norskov, J.K.; Chorkendorff, I. Bioinspired molecular co-catalyssts bonded to a silicon photocathode for solar hydrogen evolution. *Nat. Mat.*, **2011**, *10*, 434.
- 37. Majumdar. A. Structural and functional models in Mo and W bioiorganic chemistry. *J. Chem. Soc. Dalton Trans.*, **2014**, *43*, 8990.

- 37. Pergola, R.D.; Ceriotti, A. Garlaschelli, L.; Demartin, F.; Manaserro, M. Masciocchi, N. Sansoni, M. Iron-iridium mixed-metal carbonyl clusters. Synthesis, characterization and chemical behavior of [FeIr₄(CO)₁₃]²⁻ and [Fe₂Ir₄(CO)₁₀]²⁻. *Inorg. Chem.*, **1993**, *32*, 3277.
- 38. Bar-Nahum, I.; Gupta, A.K.; Huber, S.M.; Ertem, M.Z. Cramer. C.J.; Tolman, W.B. Reduction of N₂O to N₂ by a mixed valent tricopper-disulfido cluster. *J. Am. Chem. Soc.*, **2009**, *131*, 2912.
- 39. Chianelli, R.R.; Daage, M.; Ledoux, M.J. Fundamental studies of transition metal sulfide catalytic materials. *Advances In. Catalysis*, **1990**,40, 177.
- 40. Chianelli, R.R. Fundamental studies of transition metal sulfide hydrodesulfurization catalysts. *Catal. Rev. Sci. Eng.*, **1984**, *26*, 361.
- 41. Pecoraro, T.A. Chianelli, R.R. Hydrodesulfurization catalysis by transition metal sulfides *J. Catal.*, **1981**, *67*, 430.
- 42. Nanishankar, H.V.; Dutta, S.; Nethaji, M.; Jagirdar, B.R. Dynamics of a *cis*-dihydrogen/hydride complex of iridium. *Inorg. Chem.*, **2005**, *44*, 6203.
- 43. Farrar, D.H.; Grundy, K.R.; Payne, N.C.; Roper, W.R.; Walker, A. Preparation and reactivity of some η^2 -S₂ and η^2 -Se₂ complexes of Osmium. *J. Am. Chem. Soc.*, **1979**, *101(22)*, 6577.
- 44. O'Connor, J.M. Product Class 6: Organometallic complexes of iridium. In *Science of Synthesis*. Lautens, M. Thieme: Stuttgart, Germany, **2001**; Vol. 1; p. 617.
- 45. Kuwata, S.; Hidai, M. Hydridosulfido complexes of transition metals. *Coord. Chem. Rev.* **2001**, *213*, 211.

CHAPTER TWO

Synthesis of Six-coordinate Iridium(III) Thiolate Complexes

2.1. Introduction

The oxidative addition of weak acids to *trans*-chlorocarbonylbis(triphenylphosphine) iridium⁽¹⁾ often produces stable, six-coordinate complexes due the reactivity of its oxidation state and its unsaturated coordination sphere. Several of these compounds contain metal-hydride bonds, the addition of which is usually carried out via a *cis*-addition mechanism. However, it is possible to alter the reaction conditions for these processes to allow for the isolation of both the *trans* and *cis* addition products. The geometric arrangement of the isomers' substituents can be deduced from spectroscopic data though interest tends to focus on the structure of the latter. There has been a growing interest in sulfur-containing complexes due to their usefulness in hydrogenation reactions, biological pathways, along with many other applications. It is the purpose of this study to examine the coordination spheres of these types of complexes, as well as analyze the influence on the reactivity of some of these thiolate groups by transition metal alpha effects.

2.2. Experimental

The starting material, *trans*-chlorocarbonylbis(triphenylphosphine)iridium^(I), was prepared as described by Collman² and recrystallized to eliminate any side products. The IR showed a sharp peak at 1952 cm⁻¹, the v(CO) band and the ³¹P NMR a single resonance frequency at 5.32 ppm, indicating no major impurities. All solvents were distilled and dried before being stored under inert gas and every experiment was performed under an inert atmosphere as well. 4-methylbenzenethiol and thiophenol were purchased from Sigma-Aldrich

and characterized by ¹H NMR for the presence of any oxidation by-products. ¹H and ¹³C NMR were recorded on a Bruker 400 MHz AV400 spectrometer and an Agilent 300 MHz Varian Mercury spectrometer, respectively. IR spectra (KBR) were taken on a Bomem ABB Model MB100 spectrometer. UV-visible data was obtained on a Hewlett Packard 8453 spectrophotometer. All NMR data was collected using CDCl₃ as the solvent and CHCl₃ as an internal standard. Infrared spectra were obtained using a standard KBr pellet. Elemental analysis was carried on a Costech Model ECS4010 instrument, courtesy of the University of Montreal.

2.2.1. Synthesis of Hydridochlorosulfhydrylcarbonylbis(triphenylphosphine)iridium^(III), I

Three grams (0.004 mol) of Ir(CO)Cl(PPh₃)₂ are placed into a round bottom flask which is flushed with nitrogen before thirty milliliters of dichloromethane (DCM) is injected in by syringe. A Kipps apparatus is set up to generate one of starting reagents, hydrogen sulfide gas, *in situ*. This is accomplished by treating an excess of three grams of iron^(III)sulfide with approximately five milliliters of sulfuric acid (1:2) in deionized water and bubbling the gas into an acid-water trap connected to the flask that contains the previously suspended solution of the iridium complex in DCM. Upon saturation of the solution with H₂S, the yellow suspension turns a clear and colorless solution briefly before the final product begins to precipitate out as a white solid. This precipitate is collected on a filter and rinsed with twenty milliliters of cold methanol and ten milliliters of diethyl ether to give a yield of 85-90% (2.68 g) of complex I, IrHCl(SH)(CO)(PPh₃)₂. The product is spectroscopically identical to literature reports.³

$2.2.2. \ Synthesis\ of\ Hydridochloroiodocarbonylbis (triphenylphosphine) iridium ^{(III)},\ \textbf{II}$

Two grams (0.0025 mol) of compound I are placed in a nitrogen-flushed Schlenk flask and treated with twenty milliliters of dichloromethane. In a separate flask, 0.5 grams (0.002

mol) of iodine is stirred into ten milliliters of benzene until dissolution and then injected into the first flask with frequent stirring. Although complex **I** is largely insoluble in most organic solvents, upon reaction with the purple iodine solution the white precipitate turns into to a darkbrown solution that is subsequently refluxed overnight. The solvent is then stripped, and the crude product recrystallized from dichloromethane and ice-cold methanol to produce complex **II**, IrHCII(CO)(PPh₃)₂, at a yield of 55-60% (1.26 g).

2.2.3. Synthesis of Hydridochlorophenylthiolatocarbonylbis(triphenylphosphine)iridium(III), III

Three grams (0.004 mol) of Vaska's complex are placed into a round bottom flask and the flask flushed with nitrogen before thirty milliliters of benzene is injected in via syringe. Another syringe is used to inject 0.5 milliliters (0.005 mol) of thiophenol into the same flask and the yellow-orange solution is vigorously stirred overnight. The solvent is then removed *in vacuo* and the orange precipitate recrystallized from dichloromethane and cold ethanol to yield complex III, IrHCl(CO)(SC₆H₅)(PPh₃)₂, at 68-71% (2.29 g). Calcd.: C, 58.00; H, 4.07; S, 3.60. Found: C, 58.81; H, 4.12; S, 4.33.

2.2.4. Synthesis of Hydridochloro(*p*-toluenethiolato)carbonylbis(triphenylphosphine)iridium^(III), **IV**

Three grams (0.004 mol) of *trans*-chlorocarbonylbis(triphenylphosphine)iridium⁽¹⁾ are placed into a round bottom flask that also contains 4.5 grams (0.04 mol) of 4-methylbenzenethiol. The flask is flushed with nitrogen before thirty milliliters of benzene is injected by syringe and the resulting mixture left to stir overnight at ambient temperature. After removal of the solvent *in vacuo*, the light brown product is recrystallized from dichloromethane and cold ethanol to yield complex **IV**, IrHCl(CO)(SC₆H₄CH₃)Cl(PPh₃)₂, at 78-82% (2.67 g). The product

is spectroscopically identical to literature reports.⁴ Calcd.: C, 58.37; H, 4.86; S, 3.55. Found: C, 58.30; H, 4.36; S, 3.94.

2.3. Results and Discussion

Scheme 1. Synthesis of complexes I-IV from trans-Ir(CO)Cl(PPh₃)₂.

As a d⁸ transition metal, the electron configuration of Vaska's complex allows it to undergo a number of oxidative-addition reactions since low-valent, coordinately unsaturated metal complexes tend to behave as bases even toward weak acids such as thiols and alcohols (Scheme 1).⁵ Part of the versatility of this compound lies in the fact that late transition metals

help increase the nucleophilicity of bonded ligands due to the filled orbitals of the metal interacting with the lone pairs of the substituent, creating a repulsion that not only increases both their relative energies but also forces the lone pair on the ligand to be even more extensive than in thioesters. This thus displaces the electron cloud, making it a better nucleophile. If the ligand is a π -donor such as a halide ion like chloride, this in turn aids in stabilizing the transition metal's higher oxidation state. Sulfur groups in particular tend to act as effective π -donors since sulfur atoms can readily donate electron density from their p-orbitals to the d-orbitals of the metal. However, in the case for these d⁸ and d⁶ systems which bear full t_{2g} orbitals, there is actually a repulsion between the lone pairs of the sulfur atom and the metallic electrons, thereby leading to an increase in the nucleophilicity of the sulfur group. With this in mind, a goal of this study is to examine the nucleophilicity between various thiols upon coordination with iridium^(II) and iridium^(III) complexes despite to fact that π -donation from L \rightarrow M typically decreases this property.

In comparison to the other complexes that will be discussed in this section, complex **I**, hydridochlorosulfhydryl-carbonylbis(triphenylphosphine)iridium^(III), is found to be mostly insoluble in common organic solvents. In the past, this made its exact structure, along with the structures of its possible isomers, difficult to obtain by NMR. However, its crystal structure was resolved by Mueting *et. al.* (Figure 1), though at the time this group was unable to corroborate the structure via NMR spectroscopy.³ With the increase in high-field NMR sensitivity, however, we are now able to obtain evidence of not just one but at least three isomers for this product, as well as several other related complexes. These trends in isomerization will be discussed later in this chapter.

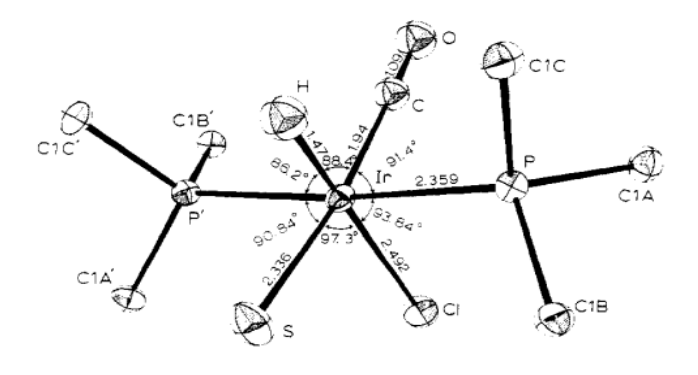


Figure 1: Structure of **Complex I** at left as assigned by Mueting, belonging to P_{21}/a space group. Note that only the ipso carbons of the triphenylphosphine groups are shown and that there is a σ-mirror plane along the S-Ir-CO bonds as well as the H-Ir-Cl bonds.

It should also be noted that at the time this structure was solved, however, there would have been no way to differentiate between the identity of the sulfur atom and that of the chloride group due to similar scattering and atomic numbers. This would have resulted in HS⁻ and Cl⁻ exhibiting similar diffraction profiles within the crystal structure resulting from their comparable electron density. This creates a real question of whether or not this structure was correctly modeled. Although the hydride occupies the vacant coordination site, its exact Ir-H separation and H-Ir-X (X = PPh₃, Cl, SH, CO) angles cannot be reliably assigned. Therefore assignment of the hydride in the structure should also be considered speculative as its position was calculated since it would be impossible to observe the diffraction of a single electron in such close proximity to an electron-dense metal center. With this discrepancy left unsettled, it was the first goal of this study to determine the structure of similar models for comparison, starting with the characterization of complex IV.

Table 1. Crystallographic data for complex **II** and **IV**.

Parameters	П	IV
Chemical formula	IrClIOP ₂ C ₃₇ H ₃₁	IrClSOC ₄₄ H ₃₈
Formula weight/g mol ⁻¹	992.03	904.39
Crystal color and habit	orange cubic	orange cubic
Crystal size/mm	0.06 x 0.06 x 0.06	0.05 x 0.05 x 0.05
Crystal system	monoclinic	monoclinic
Space group	P_{21}/n	P_{21}/c
Unit cell dimensions	- 21/	- 21/ •
a/Å	10.2255(9)	15.3911(8)
b/Å	21.9955(18)	15.2227(8)
c/Å	17.0443(14)	17.6858(9)
α (°)	90.00	90.00
β (°)	95.3790(10)	114.9440(10)
γ (°)	90.00	90.00
$V/\text{Å}^3$	3816.6(6)	
3757.2(3)	0000000	
Z	4	4
T/K	293(2)	100(2)
λ/Å	0.71073	0.71073
Density _c (g cm ⁻¹)	2.593	1.343
μ (Mo-K α)/mm ⁻¹	4.630	3.800
F(000)	1916	1800
⊕ range (°)	1.52-26.79	1.46-28.32
No. reflections collected	8103	42220
No. independent reflections	6129	8788
Δ/σ_{max}	0.003	0.001
$I > 2\sigma(I)$		
R ₁ (obs. data)	0.0766	0.0179
wR ₂ (obs. data)	0.1533	0.0437
wR ₂ (all data)	0.1685	0.0444
Goodness-of-fit on F2, S	1.048	0.975
Residual $\rho_{max}/e\mathring{A}^{-3}$	0.173	0.068

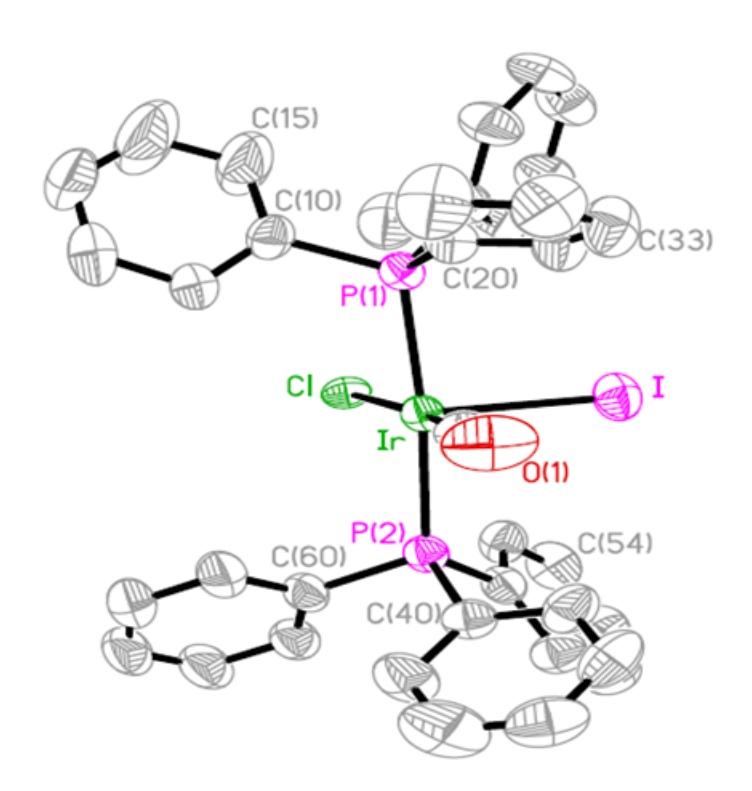


Figure 2. ORTEP drawing of complex **II**.

Table 2. Selected bond distances (Å) and bond angles (°) for complex II.

Ir-C(1)	1.844(11)	C(1)-Ir-Cl	171.2(3)
Ir-Cl	2.543(2)	I-Ir-Cl	98.44(5)
Ir-I	2.7772(7)	I-Ir-P(1)	93.68(6)
Ir-P(1)	2.367(2)	P(1)-Ir-P(2)	174.52(8)
Ir-P(2)	2.371(2)	Cl-Ir-P(1)	88.66(7)
C(1)-O(1)	1.143(12)	Ir-C(1)-O(1)	179.5(10)

The coordination geometry for complex \mathbf{II} is essentially octahedral, common for $\mathrm{Ir}^{(\mathrm{III})}$ complexes. The main distortion in the configuration stems from the slight bending of the

carbonyl, triphenylphosphine and chloride ligands toward the less sterically-hindered hydride atom and away from the electron-dense iodide ligand, hence the obtuse angle between P(1)-Ir-P(2). Strong sigma donors such as hydrides, iodides or tertiary phosphines also tend to weaken the bond trans to them since they destabilize the ground state of the bond between the metal and that ligand. Though this influence is plainly evident by spectroscopic methods, it should be noted in the lengthening of the Ir-I bond, which is quite long though not atypical or the longest of these types of iridium-iodo bonds (~2.6-2.8 Å). There is a change in stereochemistry upon addition of the iodide ion as the chloride was originally trans to the hydride. Almost all other bond angles around the metal center, particularly those between phosphine groups and adjacent ligands, are very close to orthogonal, except where slight distortions can be observed. There is an octahedral vacancy left by the presence of the hydride in Figure 2 due to the electron-rich metal obscuring presence of hydride ligand. However the presence of the hydride is easily determined through spectroscopic means as its NMR and IR characteristics are unambiguous. Metal-hydride bonds, particularly those trans to halides, are typically observed around 1.7 Å by neutron diffraction analysis.³



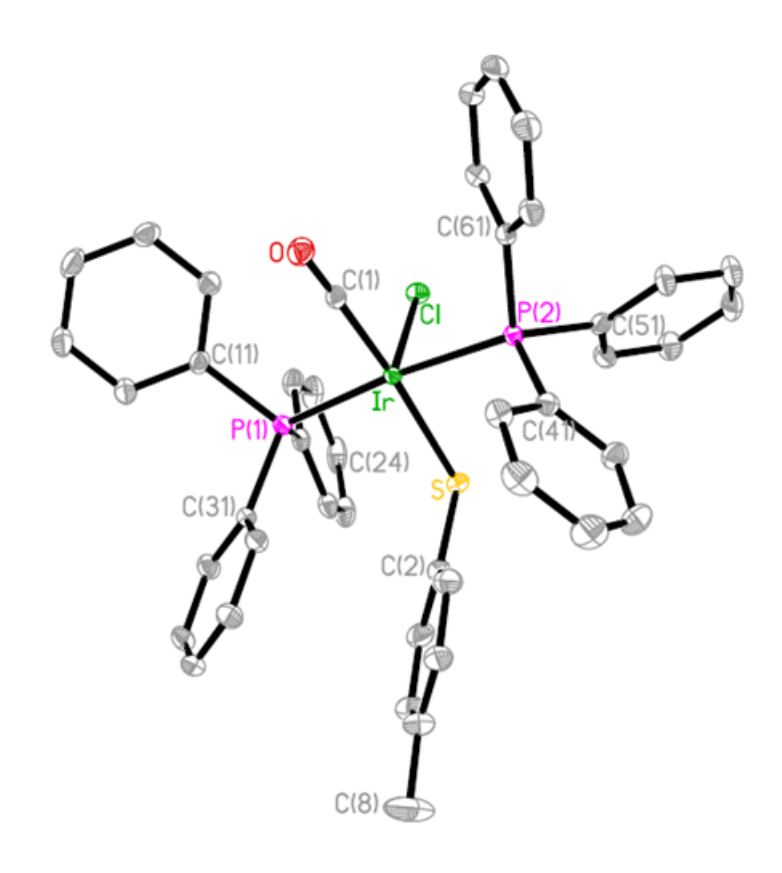
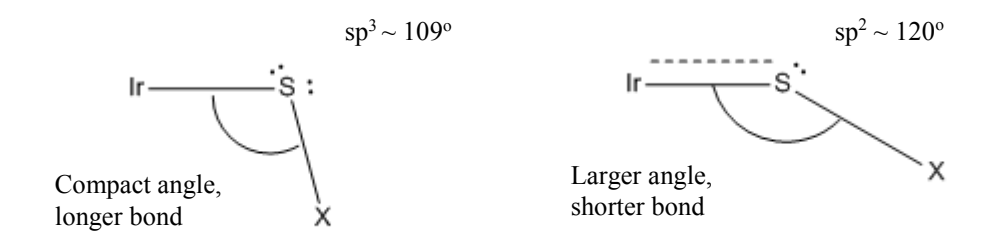


Table 3. Selected bond distances (Å) and bond angles (°) for complex IV.

Ir-C(1)	1.880(2)	C(1)-Ir-Cl	94.52(6)
Ir-S	2.4173(5)	S-Ir-Cl	93.603(17)
Ir-P(1)	2.3757(5)	S-Ir-C(1)	171.87(6)
Ir-P(2)	2.3611(5)	P(1)-Ir-P(2)	174.495(17)
Ir-Cl	2.4933(5)	C(1)-Ir-P(1)	94.28(6)
C(1)-O	1.136(2)	Ir-C(1)-O	174.67(18)
S-C(2)	1.792(2)	Ir-S-C(2)	109.21(7)

Complex **IV** would display a nearly ideal octahedral geometry except for the distortion of the structure as the PR₃, CO and *p*-tolyl thiol groups bend away toward the hydride ligand. Steric effects can also be observed in the compact Ir-S-C(2) bond angle caused by the lone pair electron clouds on the sulfur as they repel each other as well as the attached electron-dense aromatic *p*-tolyl group. The value for this angle is smaller compared to that of other iridium-thiolate complexes (~110-114°), which bear more substituted aromatic rings, and the iridium-sulfur bond distance is somewhat larger than usual (~2.3-2.4 Å).^{3,6} In comparison to the structure resolved by Mueting, both the iridium-sulfur and iridium-chloride bond lengths are larger than for complex **IV**, though the latter distance is closer to the value expected for such bonds (~2.4-2.5 Å). The difference in these values could be due to the two lone pairs on the sulfur atom, where one lone pair could donate its electron density to the iridium to become "sp²" hybridized (Scheme 2).



Scheme 2. Possible hybridization of Ir-S bonds.

This would result in a shorter iridium-sulfur bond and a wider angle around the sulfur. Halogen-substituted aromatic rings tend to pull electron-density away from the thiolate, allowing it to participate in this type of hybridization while aromatic rings with more electron-donating groups retain thiolate ligands that exhibit more "sp³" hybridized character, resulting in a longer iridium-sulfur distance and a smaller Ir-S-C(2) angle, such as that found in complex **IV**.

Both the iridium-phosphorus distances for the complex are nearly equal, and the $C_6H_4CH_3$ ring is aligned parallel to an aromatic C_6H_5 ring from the closer triphenylphospine ligand. This behavior is usually typical of pentafluorophenyl rings, SC_6F_5 , but gives rise to evidence of the packing effects in the crystal lattice structure. The Ir-S bond distance is on par with those found in many other transition-thiol complexes, especially those *trans* from weak influencers such as carbonyl groups. The iridium-chloride bond length is slightly longer than normally found though this observation is largely attributed to the strongly bound hydrido ligand *trans* to the halide. Both the structures for complexes **H** and **IV** correspond to those found for the *cis* oxidative addition products, which seems to be the predominate species of these types of reactions though compound **H** was not formed by a *cis* mechanism.

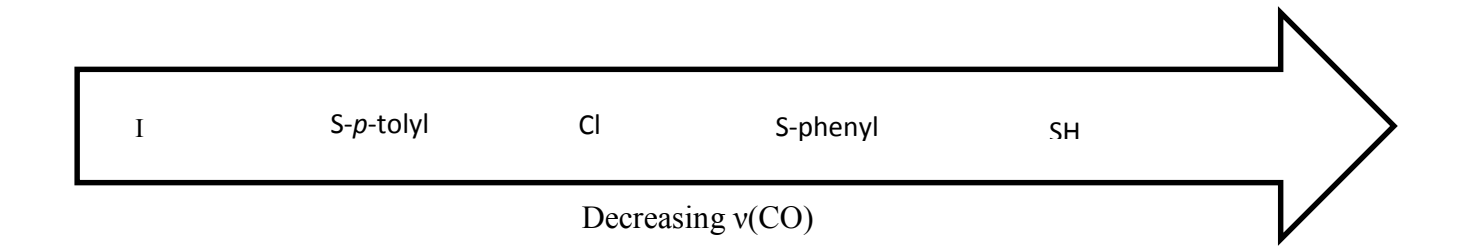
Table 4. Physical properties of compounds I, II, III and IV.

No.	Formula,	IR (cm ⁻¹)
	Color	ν(C=O)	$\nu_{sym}(\text{Ir-H})$
I ^a	IrHCl(SH)(CO)(PPh ₃) ₂ Off-white	2015(s)	2239(w)
II	IrHCII(CO)(PPh ₃) ₂ Brown	2050(s)	2206(m)
III	IrHCl(SC ₆ H ₅)(CO)(PPh ₃) ₂ Orange-Brown	2020(s)	2264(w)
IV	IrHCl(SC ₆ H ₄ CH ₃)(CO)(PPh ₃) ₂ Light Brown	2024(s)	2261(w)

^aIrHCl(SH)((CO)PPh₃)₂ also displays a peak at 2155cm⁻¹, corresponding to v(SH).

Usually oxidative-addition reactions such as these are also accompanied by a shift in the infrared band of the carbonyl group to a higher frequency as this vibration is sensitive to the oxidation state and electron density of the central metal atom. 13,14 The increase in positive charge on the metal ion tends to reduce the donation of electrons from its filled orbitals to those of the antibonding π^* -orbital of the carbonyl group, thereby strengthening the CO bond. The change on the shift of v(CO) also relies heavily on other π -substituent effects, 15 notably the difference between the high frequency of v(CO) for complex **II** compared to the others. This can be attributed to halide(p)-metal(d) π -type interactions that go on within this complex where the metal d-orbitals have more bonding character with respect to iodide due to the larger ligandmetal orbital overlaps when compared to complex **I**. Considering that complex **II** has two halide ligands dominating its coordination sphere, it is not surprising to expect the influence of the interaction between Ir(p,d) orbitals and the π^* orbitals of the carbonyl group to significantly affect the v(CO) frequency stretch to such a degree, 15 a trend made evident by Scheme 3.

Scheme 3. Trends in $\Delta v(CO)$ with respect to the anion *trans* to CO.



Typically, v(M-H) stretching modes are unobservable by infrared since they tend to be either weak or coupled with other vibrational modes of the molecule. Nevertheless every complex has bands between 2265-2235 cm⁻¹. The high values of these bands all suggest that the hydrides are *trans* to a halide ligand. This value begins to decrease with the increasing *trans*-influence of the halogen, an example of which can be seen when comparing the bands for

complex **I** and complex **II**. Though complex **I** is the precursor for the latter molecule, the mechanism which generates complex **II** causes the chloro ligand originally *trans* to the hydride to become opposite the carbonyl group while the iodo ligand takes its place across from the hydride. This in turn results in a shift of v(Ir-H) from 2239 cm⁻¹ to 2206 cm⁻¹. The change is consistent with the general trend found in literature for *trans* hydride-metal-halide stereochemistry¹⁶ though the value is usually independent with respect to the substitutions on the aromatic thiol group,¹⁷ hence only a slight difference between v(Ir-H) for complexes **III** and **IV**.

Table 5. Nuclear magnetic resonance data for complexes I, II, III and IV.

No	Isomer	¹ H NMR (CDCl ₃)	³¹ P NMR (CDCl ₃)	Average isomer
		δ-values (ppm)		ratios
$I^{a,b}$	A	-16.57(t, 1H, :H, ${}^{2}J_{P,H} = 13.0 \text{ Hz}$),	-5.38	5
		$-2.02(t, 1H, SH, {}^{3}J_{H,H} = 8.0 Hz)$		
	В	-15.24(t, 1H. :H, ${}^{2}J_{P,H}$ = 12.0 Hz),		3
		-2.11 (t, 1H, SH, ${}^{3}J_{H,H} = 8.0 \text{ Hz}$)		
	C	$-11.35(t, 1H, :H, {}^{2}J_{P,H} = 12.0 Hz),$		1
		$-2.31(t, 1H, SH, {}^{3}J_{H,H} = 8.0 Hz)$		
II	A	-13.13(t, 1H, :H, ${}^{2}J_{P,H} = 20.0 \text{ Hz}$)	-17.33	10
	В	-11.97(t, 1H, :H, ${}^{2}J_{P,H} = 20.0 \text{ Hz}$)		1
III	A	-16.34(t, 1H, :H, ${}^{2}J_{P,H} = 12.0 \text{ Hz}$),	-10.42	10
		3.46(s, 3H, CH ₃)		
	В	-15.32(t, 1H, :H, ${}^{2}J_{P,H} = 12.0 \text{ Hz}$),		3
		3.75(s, 3H, CH ₃)		
IV	A	$-16.37(t, 1H, :H, {}^{2}J_{P,H} = 24.0 Hz)$	-10.76	10
	В	-15.72(t, 1H, :H, ${}^{2}J_{P,H} = 24.0 \text{ Hz}$)		5
	C	-12.21(t, 1H, :H, ${}^{2}J_{P,H} = 24.0 \text{ Hz}$)		1

^aIn each case aromatic multiplets are observed between 7.22-7.75 ppm for all complexes. Complexes **III** and **IV** observe doublet peaks between 6.0-6.75 ppm for each isomer. ^bOther peaks were observed in the ³¹P NMR spectra but could not definitively be assigned to any specific isomers.

The proton spectra for the complexes are typical of transition metal-hydride complexes coordinated by triphenylphosphine. The high-field triplets for isomers A are consistent with hydrides being *cis* to two tertiary phosphines and *trans* to weak *trans*-influence ligand such as

chloride. The thiol proton frequency for complex **I** is considerably further downfield than the shift of the hydride. This occurrence was noted by Griffith *et al.* as a paramagnetic screening effect that tends to arise when excited electronic states become accessible, thus providing shielding to the metal nucleus as well as its neighboring hydride ligand. ¹⁸ The electron density of the metal center as well as the short Ir-H bond also helps reduce the magnetic field experienced by the hydride, causing its chemical shift to be further upfield. The coupling constants for these two protons vary greatly as well since their coupling paths are different and larger paths, *i.e.* the hydride to phosphines, result in bigger coupling constants. Sharp, single resonances found for the ³¹P NMR spectra of complexes **I-IV** arise from the magnetically equivalent phosphine groups in a mutually *trans* position. ¹¹

2.4. Isomers

For every complex mentioned in this study, at least two isomers were found via both ¹H and ³¹P NMR spectroscopy, corresponding to the structures shown in Figure 4. Though it would be difficult to determine which isomer belongs to which NMR resonances, as the coupling constants between the hydrides and the two *trans* triphenylphosphine groups are relatively similar for all four complexes. Collman *et al.*² have found in their studies that the evolution of the isomers can depend entirely on the solvent that the oxidative addition is carried out in. Using chloroform or benzene tends to favor the *cis* oxidative addition, isomers B and C exclusively, while utilizing dichloromethane or dimethylformaldehyde gives rise to both *cis* and *trans*-addition products, indicating that the polarity of the solvent plays a major role in the reaction mechanism ⁶

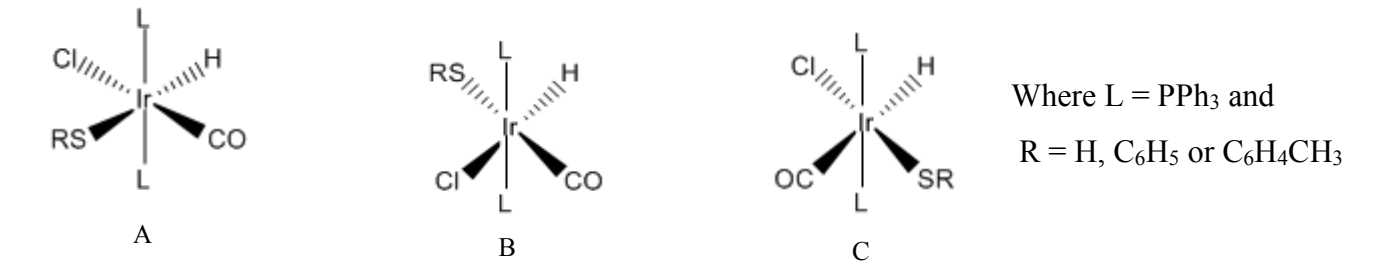


Figure 4. Possible isomers for complexes for complexes I, III, and IV.

Such isomers are also found for complex II, which most likely correlate to isomers A and C. Interconversion between these isomers is not unusual and is possibly reconfirmed by this study via ¹H NMR. Upon formation in chloroform or benzene, isomer B can be exclusively obtained though when left standing in CD₂Cl₂, presence of other species begin to arise further downfield, suggestive of hydrides trans to less trans-influencing substituents than halides such as thiols or carbonyls (isomers A and C). While it is difficult to ascertain whether or not these isomers are actually undergoing interconversion or merely yielding chlorination products with the solvent, it was noted by Stiddard⁴ that some interconverting isomers display varying bands for v(CO) and v(Ir-H), as much as $\Delta v \approx 17 \text{ cm}^{-1}$ and $\Delta v \approx 20 \text{ cm}^{-1}$, respectively. Given the difference of shifts between two isomers, it was determined that isomer B corresponded to the complexes with higher v(CO) values and decreased v(Ir-H) bands. Though the group could not isolate the crystal structure of the second isomers, it is reasonable to suggest that its structure is closer to that of isomer A than C, considering that if the hydride group was trans to the carbonyl, the hydride's influence would lower v(CO) and cause vI(Ir-H) to be higher without the transinfluence of the halide, rather than vice versa. 19

2.5. Reactivity of Complex I

Though Vaska managed to characterize complex **II** via a different reaction mechanism than the one found here, ²⁰ its facile reproduction suggests pronounced stability of complex **I**. A possible pathway for the reaction of complex **I** as it forms complex **II** is shown in Scheme 4. Originally, it was the intent of this study to substitute the hydride ion in order to decrease the lability of the sulfhydryl group, therefore increasing the reactivity of the complex. However, it was surprising to find that thiol group was cleaved rather than the hydrido group or even the chloro ligand. Usually d⁶-6-coordinate metal complexes are substitutionally inert, however similar lability of thiol ligands was observed by Singer and Wilkinson, ²¹ where upon heating, complex **II** reversibly eliminated the group to revert back to *trans*-IrCl(CO)(PPh₃)₂. The facile dissociation of RS⁻ could be due to the a slight *trans* effect of CO on the ligand, thereby labilizing it since the carbonyl's observed influence would be even stronger than that of the hydride ligand considering that CO is a strong π-backbonder.

Scheme 4. Possible reaction pathway for Complex **II**.

Acid-base experiments as well as deuterium exchange experiments were conducted to examine the properties of the terminal proton-bearing ligands of complex **I**. Dissolved solutions of the compound were treated with a stoichiometric amount of strong base in hopes of removing the proton from the sulfhydryl group due to the inherent acidity of RSH. This was accomplished

but was accompanied by a decrease in the concentration of the hydride as well, though the change in ratios is 4:1, favoring deprotonation of the sulfhydryl group first. However, upon treatment with stoichiometric amounts of acid to see if the reaction is reversible, only the hydride resonance is retained, but its upfield shift indicates loss of the sulfhydryl group. Results of these experiments can be found in Table 6, and are confirmed by MeOD and D_2O experiments where there is a major shift of $v(SH) \approx 2156$ cm⁻¹ to v(SD) = 1556 cm⁻¹ before the shift of v(Ir-H) = 2239 cm⁻¹ to v(Ir-D) = 1605 cm⁻¹. There is also an initial disappearance of the minor isomers over the major isomer in 1H NMR, which suggests that the first isomer might be more kinetically stable to these kinds of reactions.

Table 6. Spectroscopic data for complex I upon treatment with acid and base.

Functional Group	¹ H NMR(ppm)	¹ H NMR(ppm)	¹ H NMR(ppm)	¹ H NMR(ppm)
	Initial	Post NEt ₃ only	Post NEt ₃ and CF ₃ COOH	Post CF ₃ COOH only
Sulfhydryl ^a	-2.02	-2.04	Absent	Absent
	$(t, 1H, SH, ^3J_{P,H}=8.0 Hz)$	$(t, 1H, SH, ^3J_{P,H}=12.0 Hz)$		
Metal-hydride	-16.57	-16.57	-17.55	-17.62
	$(t, 1H, :H, ^2J_{P,H} = 13.0 \text{ Hz})$	$(t, 1H, :H,$ $^{2}J_{P,H} = 14.0 \text{ Hz})$	(s, b, 1H)	(s, b, 1H)

^aAll spectra were obtained using CD₂Cl₂ as the solvent.

The acidity of the metal-hydride is noteworthy though such observations can be common depending on the electronic nature of the metal and its ligand set. However, what extracts the thiol group from the complex, while retaining the hydride ligand, remains uncertain. Further examples of this phenomena are shown below in Table 7.

Table 7. Reactions of IrHCl(SH)(CO)(P(C_6H_5)
--

Compound	Solvent	ν(Ir-H), cm ⁻¹	ν(CO), cm ⁻¹	ν(new), cm ⁻¹	Observations
[NO ⁺][-BF ₄]/Na ₂ CO ₃ ^a	DCM/MeOH	2236(m)	2022(s)	1571(s)	Yellow solid
AuCl(PPh ₃) ^b	Benzene	2237(m)	2022(s)		Brown solid
$\mathrm{CS}_2{}^c$	CS ₂		2030(s)	1354(w), 1005(s) 996(s), 888(m)	Dark brown solid

All reactions were performed overnight under inert atmosphere and ambient conditions unless otherwise indicated. ^aComplex I and [NO][BF₄] were dissolved in DCM while Na₂CO₃ was added in an alcohol solution. ^bSimilar results are obtained when DCM is used as the solvent. ^cReaction was conducted under reflux and reacted with a stoichiometric amount of NEt₃.

Scheme 5. Possible reaction pathways for the reactions listed in Table 7.

For each complex mentioned in Table 7 there is the loss of $v(SH) \approx 2155$ cm⁻¹, confirmed by ¹H NMR. The reaction of complex **I** with nitrosonium tetrafluoroborate yields a new complex with a sharp band at around 1571 cm⁻¹, assigned to v(NO). Several other nitrosothiol complexes have been characterized, and the value of the band is consistent with those in the literature, ²² although additional characterization of this product is hindered by its extreme reactivity.

When compared to the oxidative-addition product of Vaska's complex and HCl, the infrared spectra of the third reaction is nearly identical, down to v(Ir-H) and v(Ir-CO). Rather than the sulfur group attaching itself to AuCl(PPh₃) through the gold atom, leading to loss of the chloride, it seems that the opposite occurred; *i.e.* the chloride ion on the gold complex displaced the original sulfhydryl ligand, allowing it to be abstracted by Au⁽¹⁾. This is not entirely unlikely given that gold and sulfur are both "soft" atoms, resulting in them having a high affinity for each other over other elements.

The product of the CS₂ reaction proved difficult to isolate as it proceeded to degrade upon recrystallization. Furthermore, the ³¹P NMR data was inconclusive due to the complex likely being paramagnetic, resulting in an absence of peaks. The ¹H NMR spectra shows the loss of both the sulfhydryl and metal-hydride protons, giving rise to possible chelation of carbon disulfide onto the complex, though paramagneticism of the complex does affect these resonances, making them appear broad.. The presence of peaks at 996 cm⁻¹ and 1005 cm⁻¹ in the infrared spectra shows evidence of what might be a thiocarbonate-type ligands since these values are consistent with those in literature for those types of complexes²³ and the bands at 1354 cm⁻¹ and 888 cm⁻¹ are related to Ir^(III)-C-S bond stretching and possibly an C=S stretching mode, respectively.

2.6. Conclusions

This series of d⁶ iridium complexes are not as kinetically stable as expected, especially compared to those in literature. In fact, the metal centers and most of their respective thiolates seem to be quite labile, easily undergoing reductive elimination and substitution. This reversible binding makes these complexes good starting materials with respect to being able to simultaneously retain hydrides, the other oxidative addition substituent. The reactivity of Complex I's sulfhydryl group was also examined and although under harsh conditions it tends to be readily abstracted, there is evidence to support that it is able to not only be retained under reasonable conditions but also react with other groups to yield even more reactive species. Further work needs to be done to investigate the nature of these phenomena and what they could mean in terms of the nucleophilicity of these late transition metal sulfur groups.

2.7. References

- 1. Douvris, C.; Reed, C.A. Increasing the reactivity of Vaska's compound. *Organomet.* **2008**, *27(5)*, 807.
- 2. Collman, J.P.; Sears, C.T. Stereochemistry of oxidative addition reactions of iridium⁽¹⁾ complexes. *Inorg. Chem.* **1968**, *7*, 27.
- 3. Mueting, A. M.; Boyle. P. Reaction of H₂S with phosphine complexes of Rh^(I) and Ir^(I). *J. Am. Chem. Soc.* **1984**, *23*, 44.
- 4. Stiddard, M. H; Townsend, R. E. Benzenethiolato-derivatives of Ir^(I) and Ir^(III). *J. Am. Chem. A: Inorg. Phys. Theor.* **1970**, 2719.
- 5. Vaska, L; Catone. D. L. A new series of four-, five-, and six-coordinate iridium complexes. *J. Am. Chem. Soc.* **1966**, *88*(*22*), 5324.
- 6. Blake, D. M.; Kubota, M. Stereochemical course of addition of hydrogen halides to iridium⁽¹⁾ complexes. *Inorg. Chem.* **1970**, *9*, 989.
- 7. Clark, G.R.; Lu, G.; Roper, W.R.; Wright, L.J. Stepwise reactions og acetylenes with iridium thiocarbonyl complexes to produce isolable iridacyclobutadienes and conversion of these to either cyclopentadienyliridium or tethered iridabenzene complexes. *Organomet.*, **2007**, *26(9)*, 2169.
- 8. Kalck, P.; Bonnet, J. Oxidative addition of halogens to thiolato-bridged dinuclear iridium^(I) complexes. *Organomet.*, **1982**, *I*(9), 1214.

- 9. El Amane, M.; Maisonnat, A.; Dahan, F.; Pince, R.; Doilblanc, R. Double oxidative addition of dihaloethane to dinuclear iridium^(I) complexes. *Organomet.*, **1985**, *4*(4), 774.
- 10. Fruzuk, M.D.; MacNell, P.A.; Rettig, S.J. Ancillary ligand involvement in the addition of dihydrogen by iridium^(III) complexes. *Organomet.*, **1985**, *4(6)*, 1144.
- 11. Antonio. A. Iridium–fluorobenzenethiolato complexes. *Polyhedron*, **1999**, *18*(11), 959.
- 12. Clark, G.R.; Russell, D.R. A chelate methyldisulphido-ligand for methylation of coordinated disulphur. *J. Organomet. Chem.* **1977**, *136*, C1.
- 13. Hsieh, M.; Zingaro, R.; Krishnan, V. The oxidative addition of selenols to Vaska's compound. *J. Sulfur Chem. A.* **1971**, *1*(3), 197.
- 14. Collman, J.P. Patterns of organometallic reactions related to homogenous catalysis. *Acc. Chem. Res.* **1968**, *1*(*5*), 136.
- 15. Abu-Hasanayn, F.; Goldman, A.S.; Krogh-Jespersen, K. Molecular Orbital study of substituent effects in Vaska type complexes. *Inorg. Chem.* **1994**, *33*, 5122.
- 16. Gaylor, J. R.; Senoff. C.V. Kinetic study of the oxidative addition of substituted benzenethiols to trans-halocarbonylbis(triphenylphosphine)iridium(I). *Can. J. Chem.* **1972**, *50*, 1868.
- 17. Birnbaum, E. R. Hydride chemical shifts in monohydrido halido transition metal complexes. *Inorg. Nucl. Chem. Lett.* **1971**, *7*, 233.
- 18. Griffith, W. P.; Orgel. L.E. The residual paramagnetism and nuclear magnetic resonance spectra of cobaltic complexes. *Trans. Faraday Soc.* **1957**, 53, 601.

- 19. Marsala, V.; Faraone, F.; Piraino, P. Facile cleavage of the P-H bond of secondary phosphine sulfides by nucleophilic Rh^(I) and Ir^(I) metal complexes. *J. Organomet. Chem.* **1977**, *133*, 301.
- 20. Vaska, L. Stereospecific addition of hydrogen halides to tetragonal d8 complexes. *J. Am. Chem. Soc.* **1966**, *88*, 5325,
- 21. Singer, H.; Wilkinson, G. Oxidative addition of HCN, H₂S and other acids to PPh₃ complexes of Ir^(I) and Rh^(I). *J. Chem. A: Inorg. Phys. Theor.* **1968**, 2516.
- 22. Perissinotti, L.L.; Leitus, G.; Shimon, L.; Estrin, D.; Doctorovich, F. A unique family of stable and water-soluble *S*-nitrosothiol complexes. *Inorg. Chem.* **2008**, *47*(11), 4723.
- 23. Kubota, M.; Carey, C.R. Intermediates in a synthesis of *trans*-IrCl(CS)(PPh₃)₂. *J. Organomet. Chem.* **1970**, *24*, 491.

CHAPTER THREE

Activated Low-valent Ir^(I) and Ir^(III) Thiolate Complexes

3.1. Introduction

Compared to the six-coordinate complexes synthesized in Chapter Two, four- and five-coordinated iridium complexes are rarer and, due to their low oxidation state and coordinative unsaturation, also much more reactive. Many of these types of complexes have the ability to reversibly bind other small molecules (XY) through oxidative addition and cleavage of the X-Y bond or by activation of the molecule while keeping XY intact. It has been found that the reactivity of these complexes bear a strong ligand-dependence with the tertiary phosphine ligands playing a major role in the reversibility of these types of reactions. Upon coordination of a small molecule and a change of oxidation state, however, several of these complexes often exhibit a higher dissociative stability when compared to that of one of the most well-known reversibly binding complexes, *trans*-Ir(CO)Cl(PPh₃)₂. The versatility of these types of complexes is discussed later in this chapter.

3.2. Experimental

The starting material for complexes I-II, $[Ir(dppe)_2(CO)]Cl$ (dppe = diphenylethane), was prepared as described by Vaska ³ and characterized by infrared and NMR spectroscopy for side products. Infrared found a sharp $\nu(CO)$ band at 1933 cm⁻¹ while ³¹P NMR found a single resonance at 28.3 ppm. The starting material for complexes III-V, $Ir(N_2)(PPh_3)_2Cl$, was prepared as described by Collman^{4,5} with a few modifications. The product was characterized for side products by infrared and NMR spectroscopy, with a sharp $\nu(N_2)$ band at 2105 cm⁻¹ and a single ³¹P NMR peak observed at about 20 ppm. All solvents were distilled and dried before being

stored under inert gas, and every experiment was performed under an inert atmosphere as well. Thiophenol, ethylene sulfide, potassium thiocyanate and 4-nitrothiophenol were purchased from Sigma-Aldrich and characterized by ¹H NMR and infrared for the presence of any oxidation byproducts. ¹H and ¹³C NMR were recorded on a Bruker 400 MHz AV400 spectrometer and an Agilent 300 MHz Varian Mercury spectrometer, respectively. IR spectra (KBR) were taken on a Bomem ABB Model MB100 spectrometer. UV-visible data was obtained on a Hewlett Packard 8453 spectrophotometer. All NMR data was collected using CDCl₃ as the solvent and CHCl₃ as an internal standard. Infrared spectra was obtained using a standard KBr pellet. Elemental analysis was carried on a Costech Model ECS4010 instrument, courtesy of the University of Montreal.

3.2.1. Synthesis of $[IrH(SC_6H_5)(dppe)_2]Cl$, I

Upon formation of [Ir(dppe)₂(CO)]Cl from Ir(CO)Cl(PPh₃)₂ after the displacement of the triphenylphosphine groups by two equivalents of dppe, the crude white product is isolated. Then 50 mg (0.0475 mmol) of [Ir(dppe)₂(CO)]Cl are placed into 10:1 solution of toluene-isopropanol, and heated at reflux at 100 °C for ten minutes. After this time, the solution turns orange, indicating the loss of the carbonyl group, and the solution is allowed to cool to room temperature before 5 μL (0.005 mmol) of thiophenol is added to the flask by syringe. Almost immediately a color change is observed as the solution turns from bright orange to pale yellow. The solvent is then stripped *in vacuo* and the yellow product recrystallized from benzene and hexanes to yield complex **I** in 70% yield (39 mg). Calcd.: C, 64.94; H, 5.39; S, 2.32. Found: C, 64.44; H, 5.23; S, 2.37.

3.2.2. Synthesis of [IrH(SC₆H₄NO₂)(dppe)₂]Cl, II

Similar to the preparation of complex **I**, complex **II** is formed by treating a warm solution of [Ir(dppe)₂]Cl (50 mg, 0.05 mmol) in toluene-isopropanol (10:1) with 8 mg (0.052 mmol) of 4-nitrothiophenol and then allowing the solution to stir for one hour. After this time, the original orange solution becomes a deep red. Upon stirring the solvent and recrystallizing the crude product from benzene-hexanes, the final product is isolated in 85% yield (49 mg). Calcd.: C, 60.04; H, 4.77; S, 2.86; N, 1.25. Found: C, 59.43; H, 4.90; S, 2.60; N, 1.18.

3.2.3. Synthesis of IrHCl(SC₆H₅)(PPh₃)₂, III

The starting reagent, *trans*-Ir(N₂)Cl(PPh₃)₂, is prepared and 50 mg (0.064 mmol) placed into a flask and dissolved in 10 mL of benzene before 6.5 μL of thiophenol is added by syringe. The solution is stirred overnight to allow the originally yellow-green solution to become orange, the color change indicating the oxidation state change of the metal. The solvent is stripped and complex **IV** isolated by recrystallization with benzene and hexanes with a final yield of 55% (30 mg). Calcd.: C, 58.49; H, 4.21; S, 3.72. Found: C, 59.35; H, 4.17; S, 4.04.

3.2.4. Synthesis of IrHCl(SC₆H₄CH₃)(PPh₃)₂, **IV**

Complex **IV** is prepared by the same method as complex **III** with the exception of using 8 mg (0.064 mmol) of 4-methylbenzenethiol. The final product is obtained from recrystallization with benzene-hexanes to yield an orange-brown solid at 67% yield (38 mg). Calcd.: C, 58.93; H, 4.37; S, 3.66. Found: C, 58.02; H, 4.20; S, 3.83.

3.2.5. Synthesis of Ir₂Cl₂(SC₂H₄)₂(PPh₃)₄, V

Approximately 50 mg (0.064 mmol) of *trans*-Ir(N₂)Cl(PPh₃)₂ is placed into a flask and dissolved in 10 mL of benzene. Using a syringe, 4 μ L (0.064 mmol) of ethylene sulfide is injected into the flask. The yellow-green solution is allowed to stir overnight to yield a pale yellow suspension. The solvent is removed and the crude product recrystallized from benzene and hexanes with a yield of 60% (31 mg). Calcd.: C, 56.18; H, 4.22; S, 3.95. Found: C, 56.92; H, 4.34; S, 4.16.

3.3. Results and Discussion

The cationic species of iridium in this study tend to exhibit increased reactivity when compared to that of their parent complex, Ir(CO)Cl(PPh₃)₂. One contrast of note is the higher dissociative stability [Ir(CO)(dppe)₂]Cl upon coordination of a small molecule such as O₂. While Vaska's complex is relatively stable under ambient conditions, the latter tends to be readily oxidized by air when left standing, converting from a white solid to a cream-colored product that has an infrared peak at 845 cm⁻¹, suggestive of an iridium-bound v(O₂) stretch. While this addition can be reversibly eliminated for Vaska's complex by bubbling an inert gas such as N₂ through a solution of it, [Ir(O₂)(dppe)₂]Cl must be placed under vacuum for several hours or heated in order to abstract the molecule, indicating the greater stability of the compound.³ Also, unlike Vaska's complex, the other complex also loses the carbonyl group upon binding of O₂, rather than retaining both molecules, where a loss of v(CO) band at 1933 cm⁻¹ is observed.

This reactivity is due to low-valence of the complex and its octahedral vacancy, leading to a pronounced facile oxidative-addition of weak acids.³ The presence of the dppe chelate further increases the electron density on the metal since it is a stronger donor than

triphenylphosphine.² Vaska found that this dissociative reaction rate is increased when correlated with the latent basicity of the certain metal complexes as the tertiary phosphine groups become more electron-dense (*i.e.* P(aryl)₃ versus P(alkyl)₃. There is also evidence of steric factors coming into play in complexes containing the bisphosphine chelate, a trend noted by Reed *et al.*¹, where complexes containing bulkier tertiary phosphine groups, regardless of electronic nature, tend to favor coordination unsaturation when compared to molecules with less sterically-hindered ligands. These types of d⁸ systems, particularly those coordinated by dppe, tend to exhibit square planar geometry at the expense of distorting the ethane bridges, a fact supported by ¹H NMR⁶ as well as the studies of complexes **I-II**.

Cationic complexes are not the only compounds to undergo reversible molecular binding, however,² since molecules such as SO₂ and HCN reversibly form adducts with even neutral complexes, nor are cationic complexes the only compounds to form coordinately unsaturated thiolate derivatives.^{7,8} Vaska's complex, upon displacement of its carbonyl group with a dinitrogen group from an acid azide, has been reacted with several molecules^{4,9} such as carbon disulfide and diethyl maleate due to the extreme lability of N₂ in both air and solution. Reactions of this type are becoming more commonplace but it was the goal of this study to ascertain if five-coordinate complexes could therefore be obtained through oxidative addition of Ir(N₂)Cl(PPh₃)₂. These results for these reactions, complexes III-V, are shown in the tables below.

Table 1. Physical properties of compounds **I-V**.

No.	Formula,	IR ((cm ⁻¹)
	Color	ν(Ir-H)	ν (other)
I	[IrH(SC ₆ H ₅)(dppe) ₂]Cl Yellow	2204(w), 879(m)	
II	[IrH(SC ₆ H ₄ NO ₂)(dppe) ₂]Cl Red	2208(w), 878(m)	1581(s), 1335(m)
III	IrHCl(SC ₆ H ₅)(PPh ₃) ₂ Orange-brown	2275(w), 866(w)	
IV	IrHCl(SC ₆ H ₄ CH ₃)(PPh ₃) ₂ Orang-Brown	2185(w), 902(w)	
V	IrCl(SC ₂ H ₄)(PPh ₃) ₂ Yellow		638(m)

The infrared spectra for many of these compounds are simple, observing aromatic C-H stretching peaks from their tertiary phosphine groups between 3200-3000 cm⁻¹ and similar aromatic peaks from their respective thiol groups in the range of 2950-2800 cm⁻¹. Those containing hydrides such as complexes **I-IV**, have weak v(IrH) stretching between 2275-2185 cm⁻¹, typical of hydrides bound to a metal center. The spectrum of complex **II** contains at least two more distinctive peaks, one at 1581 cm⁻¹ due to v(NO₂)_{asy} and another at 1335 cm⁻¹ from v(NO₂)_{sym}. From this spectrum it is easy to distinguish whether the complex has bound to either the nitro group or thiol group of 4-nitrothiophenol as there would be a shift in v(CN) if the nitro group were activated. ¹⁰⁻¹³ Instead a change in v(CS) is observed, where it shifts to 645 cm⁻¹. The

vibration v(CS) is also visible in the spectrum for complex V at 638 cm⁻¹. The pathways for the formation of these complexes are shown in Schemes 1 and 2.

Where
$$R = H$$
, NO_2 and $L = P$

$$R \longrightarrow SH$$

$$R$$

Scheme 1. Pathways for the reaction of $[Ir(dppe)_2]Cl$ with thiolates to form complexes I and II.

Scheme 2. Pathways for the reaction of $Ir(N_2)Cl(PPh_3)_2$ with thiolates to form complexes III, IV (bottom) and V (top).

Table 2. Nuclear magnetic resonance data for complexes I-V.

No	Isomer	¹ H NMR (CDCl ₃)	³¹ P NMR (CDCl ₃)	Average isomer
		δ-values (ppm)		ratios
$\overline{\mathbf{I}^a}$	A	$-19.92(p, 1H, :H, {}^{2}J_{P,H} = 12.0 Hz),$	17.56	4
		2.30(sb, 4H, C ₂ H ₄), 2.73(sb, 4H, C ₂ H	[4)	
	В	-16.24(p, 1H. :H, ${}^{2}J_{P,H}$ = 12.0 Hz),	-12.55	1
		2.95(sb, 4H, C ₂ H ₄), 4.10(sb, 4H, C ₂ H ₄)	4)	
II		-19.91(p, 1H, :H, ${}^{2}J_{P,H} = 12.0 \text{ Hz}$),	21.03	
		$7.64(d, 2H, Ar, {}^{3}J_{H,H} = 8.0 Hz),$		
		$8.21(d, 2H, Ar, {}^{3}J_{H,H} = 8.0 Hz)$		
		2.38(sb, 4H, C ₂ H ₄), 2.85(sb, 4H, C ₂ H ₄)	4),	
III	A	-24.19(t, 1H, :H, ${}^{2}J_{P,H} = 16.0 \text{ Hz}$)	28.94	1
	В	$-23.36(t, 1H, :H, {}^{2}J_{P,H} = 16.0 Hz)$	-0.27	5
IV	A	$-24.15(t, 1H, :H, {}^{2}J_{P,H} = 20.0 Hz)$	-2.96	1
	В	$-19.39(t, 1H, :H, {}^{2}J_{P,H} = 22.0 Hz)$	28.84	4
V^b		3.15 (m, 4H, C_2H_4 , $^3J_{H,H} = 20.0 Hz$)	43.27	

^aIn each case phenyl phosphine aromatic multiplets are observed between 7.02-7.78 ppm for all complexes. The aromatic peaks of the thiol group are therefore obscured for complexes **I**, **III**, and **IV**. ^bThe protons for the ethylene bridges and the protons for the triphenylphosphine groups integrate in 1:10 ratio.

Similar to the complexes described in Chapter Two, the majority of the compounds in this chapter form isomers upon oxidative addition. This is not surprising for complex I

considering the chloride atom in its outer sphere may substitute for the thiolate ligand (Scheme 2) since these types of ligands have been found to be quite labile in Chapter Two.

In comparison, complex II only forms one isomer, probably due to the repulsion of the chloride anion and the negative charges on the nitro group of the thiol. All complexes besides V observe high-field proton shifts characteristic of hydrides attached to shielding metal centers, observable as either pentets when coupled to two equivalent dppe ligands (complexes I and II) or as triplets when coupled to two equivalent triplenyl phosphine groups (complexes III-IV). With the absence of the nitrogen group on the metal center upon formation of complexes III and IV, it is possible that either the hydride or the thiolate group coordinated trans to the chloride ligand (Scheme 2), where isomers 1A correspond to the former. This would result in a slight trans influence on the Ir-H bond, lengthening it so that the hydride is not as shielded, causing its resonances to be more down-field (isomer 1B) than the other isomer. 14 Though hydrides tend to exhibit strong trans influence themselves, their NMR chemical shifts also depend on the electronegativity of the ligand across from them as well as strong σ -donors cause $\delta(IrH)$ and v(IrH) to decrease. 15 It is worthy to note that this is predominate isomer since similar complexes usually have the thiolate group trans to the chloride instead, but this difference could be due the steric hindrance of the triphenylphosphines if the bulky aromatic thiol group was kept in the equatorial position with respect to the metal center rather than in the axial position.

Considering that there is an octahedral vacancy in the structure proposed in Scheme 2 for the formation of complexes **III** and **IV**, it would not be unusual for them to dimerize to rectify this coordinate unsaturation, shown by the second pathway (isomers 2A and 2B). It would be difficult to prove this structure by elemental analysis since both the proposed structures would have similar composition, but it is telling that for either structures that the triphenyl phosphine

ligands would remain within the same electronic environments, resulting in a single ³¹P NMR frequency, and the hydrides would also still experience the same coupling patterns to these groups as well, resulting in the triplets seen in Table 2.

For complex **V** the ¹³C NMR has three doublets between 133.57, 133.09 and 129.98 ppm as well as a singlet at 129.79 ppm, consistent with shifts typically found for triphenylphosphine ligands. This spectrum also has another singlet further upfield at 31.03 ppm and a doublet at 2.35 ppm, corresponding to the ethylene carbons closest to the sulfur atoms and the ethylene carbons closest to the metal centers, respectively. It is not unusual that only a single species is observed by ³¹P, ¹H and ¹³C NMR since the all four triphenylphosphine groups are in the same electronic environment and the same could be said for the ethylene bridges' carbons and protons as well. This complex was proposed as a dimer considering it does not readily decompose in air like many other six-coordinate iridium complexes. It does not coordinate CO upon carbonylation under prolonged reaction time in solution, indicating that it is a coordinately saturated structure, and the multiplet seen in the ¹H NMR spectrum is indicative of multiple ethylene protons coupled to tertiary phosphines.

2.4. Conclusions

Oxidative addition and reductive elimination transformations are key processes in the examination of metal complexes with respect to their reactivity. While the latter leads to electron-rich, coordinately unsaturated complexes in low oxidation states, addition products tend to be easier to study due their stability allowing for fuller characterization. When there is a vacancy left in the coordination sphere of these complexes it is possible for them to coordinate even weakly acidic molecules with the possibility of also forming isomers. While further

investigation is needed to determine the exact conditions that could shift the equilibrium between these isomers, their presence is at least telling of the configuration geometry these compounds undertake upon formation.

2.5. References

- 1. Reed, C.A.; Roper, W.R. The iridium^(I) cation, [Ir(CO)(CH₃CN)(PPh₃)₂]⁺, and its substitution reactions. *J. Chem. Soc. Dalton.* **1973**, 1365.
- 2. Vaska, L. The role of phosphorus ligands in the reversible activation of small molecules by metal complexes. *Phosphorus, Sulfur and Silicon*. **1990**, *49/50*, 437.
- 3. Vaska, L.; Catone, D.L. A new series of four-, five-, six-coordinated iridium complexes. *J. Am. Chem. Soc.* **1966**, *88*(*22*), 5324.
- 4. Collman, J.P.; Kang, J.W. Iridium complexes of molecular nitrogen. *J. Am. Chem. Soc.* **1966**, 88(14), 3459.
- 5. Collman, J.P.; Hoffman, N.W.; Hosking, J.W. *trans*-chloro(nitrogen)-bis(triphenylphosphine)iridium^(I). *Inorg. Synth.* **1970**, *12*, 8.
- 6. Ibekwe, S.D.; Taylor, K.A. Hydridoalkoxycarbonyl complexes of iridium. *J. Chem. Soc., A: Inorg. Phys. Theor.* **1970**, 1.
- 7. Antinolo. A.; Fonesca, I.; Ortiz, A.; Rosales, M.J.; Sanz-Aparico, J.; Terreros, P.; Torrens, H. Iridium–fluorobenzenethiolato complexes. *Polyhedron*, **1999**, *18(11)*, 959.
- 8. Dilworth, J.R.; Moraes, D.; Zheng, V. Rhodium and iridium complexes with thiolate and tertiary phosphine ligands. *J. Chem. Soc., Dalton Trans.* **2000**, 3007.
- 9. Kubota, M.; Carey. C.R. Intermediates in a synthesis of *trans*-Ir(CS)Cl(PPh₃)₂. *J. Organometal. Chem.* **1970**, *24*, 491.

- 10. Lin, Y-Z.; Wu, J-G.; Xu, G-X. FT-IR studies on the bonding mode of NCS groups in some new thiocyanate complexes. *Microchim. Acta.* **1988**, *94*(*1*), 219.
- 11. Mitchell, P.C. H.; Wiliams, R.J.P. The infrared spectra and general properties of inorganic thiocyanates. *J. Chem. Soc.* **1960**, *5*, 1912.
- 12. Kharitonov, Y. Y.; Rozanov, I.A.; Tananaev, I.V. Infrared absorption speactra of thiocyanate complexes of Hf^(IV). *Izvestiya Akademit Nauk SSSR.* **1963**, *4*, 596.
- 13. Lieber, E.; Rao, C.N.R.; Ramachandran J. The infrared spectra of organic thiocyanates and *iso*thiocynates. *Spectrochim. Acta.* **1959**, *13*, 296.
- 14. Olgemoller., B.; Beck, W. Correlation between the trans influence of a ligand L and the electronegativity of the donor atom in a series of hydridoiridium^(III) complexes, *trans*-H(L)Ir(CO)Cl(PPh₃)₂. *Inorg. Chem.* **1983**, *22*, 997.
- 15. Talyor, R.C.; Young, J.F.; Wilkinson, G. Hydrido and carbonylhydrido complexes of iridium containing stannous chloride. *Inorg. Chem.***1966**, *5*(*1*), 20.
- 16. Grushin, V.V. Reductive elimination of HCl from chloro hydrido transition metal complexes. *Acc. Chem. Res.* **1993**, *26*, 279.

CHAPTER FOUR

Compounds with Sulfur-rich Ligands

4.1 Introduction

Sulfur-rich ligands have been of interest in both the organic and inorganic disciplines of chemistry on account of their ability to form analogous of dithiocarboxylates, analogs of carboxylic acids (Figure 1).



Figure 1. Structure comparison of analogous carboxylate (1) and dithiocarboxylate (2) groups, shown with electron delocalization where R = alkyl, aryl group.

As outlined in Chapter 1, several proteins clusters containing sulfur and transition metals such as Fe, Zn or Cu tend to play major roles in many biological functions, *i.e.* redox transformations and electron transport. Metal sulfide chemistry has also gained increased relevance in both industrial and materials chemistry due to hydrocarbon desulfurization, the discovery of the superconductivity of some metal complexes and the effectiveness of some dithiolates as antifungal reagents in agricultural applications. Sulfur chelates also have to ability to undergo oxidation to yield disulfides and tend to be more relatively stable then other

oxygenated-derivatives, allowing for better analysis of organic compounds since these do not decompose as easily. Recently there have been many cases of sulfur-containing heterocycles being able to reversibly add and eliminate sulfur atoms, permitting better investigation into the dynamics of the ring-opening mechanism as well as the kinetics that drive such reactions.^{3,4} In this chapter the reactivity and characterization of Zn and Ni sulfur complexes, along with their chelates, are investigated with emphasis on the changes in these properties upon sulfur abstraction.

4.2 Experimental

Most chemicals in this research were prepared via known literature procedures or were purchased commercially of reagent grade and used without further purification. Tetrahydrofuran was dried and distilled over sodium-potassium amalgam under inert gas. Ammonium sulfide was prepared by commonly known methods in 25-40% aqueous solution. Methylene chloride, chloroform and hexanes were degassed by standard techniques. All products were checked for purity via thin layer chromatography or similar analytic methods. All melting points were measured by differential scanning calorimetry. H and Hand NMR were recorded on either a Bruker 400 MHz AV400 spectrometer or an Agilent 300 MHz Varian Mercury spectrometer. Infrared spectra (KBr) were taken on a Bomem ABB Model MB100 spectrometer. UV-visible data was obtained on a Hewlett Packard 8453 spectrophotometer. Differential scanning calorimetry measurements were carried out on a TA Instrumentals DSC 2010 instrument and all mass spectrometery calculations were run on a Kratos MS25RFA high-resolution mass spectrometer. Elemental analysis was carried on a Costech Model ECS4010 instrument, courtesy of the University of Montreal. Compound I, bis(p-perthiotoluato)zinc(II), compound II, bis(p-

dithiotoluato)zinc(II) and compound III, perthiotoluatodithiotoluatonickel(II) were prepared as described by Fackler⁶ *et al.* and Bruni *et al.*⁷ with a few minor modifications.

4.2.1. Synthesis of bis(p-perthiotoluato)zinc(II), Zn(S₃CC₇H₇)₂, I

Six mL (0.05 mol) of *p*-tolualdehyde is added to 13 mL solution of (NH₄)₂S in 25 mL of tetrahydrofuran along with 1.5 g (0.005 mol) of sulfur. This mixture is refluxed for about 15 minutes with constant stirring before the subsequent dark red solution is diluted with 50 mL of water and then extracted by 100 mL of ether. The aqueous phase of the mixture is then filtered and added to a solution of zinc(II)chloride hexahyd5rate (5 g in 50 mL of water). Almost instantaneously an orange precipitate begins to form which is then filtered and washed with methanol. This pasty product is redissolved in 10 mL of tetrahydrofuran to separate it from any zinc oxide impurities and filtered again, followed by the removal of the solvent via vacuum. This solid can be recrystallized from carbon disulfide and ice-cold absolute ethanol and isolated in a yield of 56% (5.32 g) with a melting point range of 192.5-194 °C. The product is spectroscopically identical to literature reports.^{6,7}

4.2.2. Synthesis of bis(p-dithiotoluato)zinc(II), Zn(S₂CC₇H₇)₂, II

Bis(*p*-perthiotoluato)zinc(II), 0.5 g (0.001 mol), is dissolved in 10 mL of benzene and treated with 1 g (excess) of tricyclohexylphosphine. The mixture is brought to reflux and then cooled to room temperature before being layered with 15 mL of ice-cold pentane. Upon further cooling a white precipitate, tricyclohexylphosphine sulfide, forms. This solid is filtered from the mixture and an additional 10 mL of pentane added to the solution. When some of the pentane is removed under vacuum a yellow precipitate begins to form which is then isolated and washed

with cold methanol. The yield is almost quantitative, 80% (0.34 g) with a melting point range of 206.5-209 °C. The product is spectroscopically identical to literature reports.^{6,7}

4.2.3. Synthesis of perthiotoluatodithiotoluatonickel(II), Ni(S₃CC₇H₇)(S₂CC₇H₇), III

One gram (0.002 mol) of compound **I**, bis(*p*-perthiotoluato)zinc(II), is dissolved in 20 mL of carbon disulfide and reacted with an excess of 0.55 g (0.0025 mol) of NiBr₂*6H₂O in 25 mL of absolute ethanol, with moderate stirring. Within moments the original orange solution becomes a deep violet color. The solvents are then removed *in vacuo* and the precipitate recrystallized from carbon disulfide and ice-cold absolute ethanol to produce a product with a melting point of 220-221.5 °C with a yield of 70% (0.64 g). The product is spectroscopically identical to literature reports.^{6,7}

4.2.4. Synthesis of methylene bis(dithio-4-methylbenzoate), IV

About 0.5 g (0.001 mol) of bis(*p*-perthiotoluato)zinc(II) is dissolved in 6 mL of methylene chloride and then treated with 550 μ L (0.002 mol) of 40% tetrabutylammonium hydroxide, N(C₄H₉)₄OH. The resulting dark red solution is allowed to stir for about ten minutes before being rinsed with 10 mL of water to removed excess zinc hydroxide. The organic phase is then extracted, layered with hexanes and set to cool at -25 °C for seven days. During this time pink-red crystals form which are isolated and washed with ice-cold water, followed by methanol to yield the structure given in Figure 3, yield 60% (0.23 g). MP: 178-179 °C; Δ H_f \approx 33.8 kJ/mol; MS (*m/z* calculated) 348.5 (M⁺), (*m/z* observed) 348 (M⁺). Calcd.: C, 58.58; H, 4.63; S, 36.80. Found: C, 57.69; H, 4.80; S, 36.94.

4.3. Results and Discussion

Scheme 1. Pathways for the formation of compounds **II-IV** from complex **I**.

Though the IR spectra patterns of compounds **I, II** and **III** appear similar, significant differences among them can be observed. Camus *et al.*⁸ found that the values for v(C=S)_{asym} for dithiocarboxylates tend to be shifted close to 15 cm⁻¹ toward lower frequencies than for the perthiocarboxylate derivatives. This is evident in the data given in Table 1 where only one stretching frequency can be seen for symmetric complexes such as **I** while complexes with non-equivalent ligands such as **III** have two bands between 1100-900 cm⁻¹ associated with non-coordinated C=S bonds, with the band appearing about 1031 cm⁻¹ corresponding to the dithio

chelate. This split in bands is not only suggestive of the difference of the ligands but reconfirmed by the presence of a single peak around 445 cm⁻¹ for complex **III**, due to a S-S vibrational band. While two peaks can be observed in this region between 490-430 cm⁻¹ for complex **I**, this large dipole moment change in the S-S bond vibration within the cyclic structure is only seen for one other complex. These multiple stretching modes are not unusual for mixed ligand complexes, MS_xS_y, indicative of the chelate ring being expanded by the presence of an additional sulfur atom, with the complex forming both a four-membered and five-membered ring (Scheme 1).⁹

As reported by J.P. Fackler *et al.*¹⁰ the disulfide sulfur atom adjacent to the phenylic carbon is quite labile, with its abstraction by tertiary phosphine groups proceeding quickly following second-order kinetics (black sulfur atoms in Scheme 1). This mechanism appears to be kinetically-controlled with the phosphine breaking the disulfide linkage so as chelate ligands lose a sulfur atom converting from five-membered rings to the four-membered form, the newly formed bond between the remaining sulfur atom and the metal ion is made more stable (red sulfur atoms in Scheme 1). This stability could possibly be the reason for the increase in this stretching frequency, however since bands within rings tend to be delocalized it can be difficult to determine bond strength from a single bond mode.

The ESMS analysis for compound **IV** has three peaks. The first peak at 348 m/z is due to the parent molecule, compound **IV**, while the latter two are the fractionated pieces of the molecule. A significant peak at 181 m/z corresponds to methylene dithio-4-methylbenzoate, while the last peak at 135 m/z belongs to the missing second dithio ligand. It should be noted however, that the second fraction is lighter than expected by 32 m/z, indicating that a sulfur atom from the ligand was abstracting during ionization. This result can be considered as tantamount to further evidence as to the lability of this sulfur atom in the chelate ring.

Table 1. Physical properties of compounds I-IV.

No.	Formula,	IR (cm ⁻¹)			UV/	Vis(nm)(CHCl ₃)
	Color	$v_{as}(C=S)$	$\nu_{\text{sym}}(CS_2)$	ν(C-S)	ν(S-S)	$\lambda_{max} (M^{-1} cm^{-1})$
Ι	Zn(S ₃ CC ₇ H ₇) ₂ Red-orange	1005(s)	1238(s)	636(w)	462, 451(m)	439(271400), 346(25700)
II	$Zn(S_2CC_7H_7)_2$ Yellow	1006(m)		635(w)		396(53200), 291(41500)
III	Ni(S ₂ CC ₇ H ₇)(S ₃ CC ₇ H ₇) Violet	1007,1031(s)	1266(s,b)	634(w)	445(m)	534(182800), 343(28300)
IV	$CH_2(S_2CC_7H_7)_2$ Pink	1017(s)		638(w)		486(637500), 312(23400)

Considering the range of colors compounds **I-IV** display, it was expected that their UV-visible absorption spectra would be highly variable as well, as shown by Table 1. While all the compounds absorb strongly between 350-260 nm due the presence of their conjugated, aromatic rings resulting in π - π^* transitions, a second band also appears for each at a longer wavelength. These visible bands correspond to the $n(p) \rightarrow \pi^*$ transition for the RCS₃ fragment of the ligands, although extensive delocalization is expected to occur. For complexes **I** and **III** the pi-conjugated systems are large due to the presence of the disulfide linkage which then narrows the energy gap between electronic transitions, giving rise to light absorption at longer wavelengths, as observed by Kato *et al.* in their studies of bis(thioacyl) sulfides. ¹¹ For example, the intense band seen at 534 cm⁻¹ for complex **III** can therefore be assigned to a metal-to-ligand-charge-transfer (MLCT) observed for many dithiolate complexes. ¹²

Compound **IV** by comparison has UV-visible absorptions at a longer wavelength than the previous two complexes. This is not surprising that the energy transitions in this compound change upon formation as this will also affect its electronic structure, confirmed by NMR.¹³ It can be speculated that there is a transition of the free lone pairs of electrons on the compound's non-conjugated sulfur atoms up to a π^* antibonding molecular orbital. This orbital is higher in energy than the highest π bonding orbitals, causing the transition to correspond to a shorter wavelength compared to complex **III**. This transition is not as intense for complex **II**, however, due to the presence of the metal ion and its affinity for electron density though the optical transitions for all these compounds remain fairly constant (between 20-50 nm) for those that bear similar ligands.

Table 2. Nuclear magnetic resonance data for compounds I-IV.

No.	¹ H NMR (CDCl ₃)
	δ-values (ppm)
I	2.45 (s, 6H, CH ₃), 7.26 (d, 4H, Ar, $J_{H.H}$ = 8.0 Hz), 8.19 (d, 4H, Ar, $J_{H.H}$ = 8.0 Hz)
II	2.46 (s, 6H, CH ₃), 7.26 (d, 4H, Ar, $J_{H,H}$ = 8.0 Hz), 8.36 (d, 4H, Ar, $J_{H,H}$ = 8.0 Hz)
III, ring A	2.39 (s, 3H, CH ₃), 7.22 (d, 2H, Ar, $J_{H,H}$ = 8.0 Hz), 7.83 (d, 2H, Ar, $J_{H,H}$ = 8.0 Hz)
III, ring B	2.43 (s, 3H, CH ₃), 7.30 (d, 2H, Ar, $J_{H,H}$ = 8.0 Hz), 8.01 (d, 2H, Ar, $J_{H,H}$ = 8.0 Hz)
IV	2. 40 (s, 6H, CH ₃), 5.36 (s, 2H, CH ₂), 7.20 (d, 4H, Ar, $J_{H,H}$ = 8.0 Hz),
	7.95 (d,4H, Ar, $J_{H,H}$ = 8.0 Hz)

The ¹H nuclear magnetic data for these compounds are displayed in Table 2. For systems that have equivalent ligands such as compounds **I**, **II** and **IV**, the spectra are simple, with the aromatic protons giving two sets of sharp doublets and single peak for their methyl groups, and in the case of compound **IV** another singlet for the central methylene protons. The simplicity of

these spectra can be assumed to be due to the uniformity of the electronic environments for each ligand, allowing their resonances to be chemically equivalent. While it is hard to distinguish perthio and dithiocarboxylates by NMR alone, the difference between the effect of the four- or five-membered ring they belong to on the adjacent aromatic protons is apparent, as also found by Mas-Balleste *et al.*¹ For example, while two sets of proton resonances that appear at 2.45 ppm (methyl) and 7.26 ppm (aromatic) remain the same for complexes I and II, upon abstraction of a sulfur atom the other set of frequency changes, shifting down-field from 8.19 ppm to 8.36 ppm, respectively. This difference can be seen in Figure 2, where protons B and B' correspond to the unchanged resonance frequencies and protons A and A' correspond to the shifted frequencies due to the change in the electron environment since they are closer to the carbon-sulfur bonds present.

Figure 2. Partial ligand structures of complexes I and II.

This phenomena is even more evident for complex **III**, which contains both a dithio-(ring A) and perthio- (ring B) chelates. Though the resonance frequencies for this complex fall very close together it is easy to see that all the protons for each ligand are in different, distinguishable environments. It should be noted, however, that the sharpness of the doublets that corresponding to protons A and A' for is both temperature and solvent-dependent for complex I and part of complex III (ring B). At 25°C in either CDCl₃ or CD₂Cl₃ this peak is a broad singlet that only splits at increased temperatures, or if the solvent is changed to another polar, aprotic solvent such as dimethylsulfoxide. This broadening was not observed for complex II, ring A for complex III or compound IV, leading to the conclusion that there is a rotational barrier for protons A and A' as a result of the nearby, influencing perthiclate group.

Although ¹³C NMR would have been more conclusive as to the nature of these environmental effects, this data was unable to be obtained due to resonances of weak intensity for the CS₃ and CS₂ carbons as also experienced by Pellizier *et al.*¹⁴ Though this group was only able to yield some tentative data which aided them to resolve many of their structures, they were also able to observe the difference in functional groups due to the strong deshielding substituent effect caused by their central metal ion, Cu^(II). However, for this research complex **III** was reacted with triphenylphosphine to abstract the terminal sulfur atom from the disulfide linkage of ring B to yield resonance frequencies that fell into the range originally observed for ring A, allowing for differentiation between the two sets of proton frequencies.

4.4. Preparation and Structural Analysis for Compound IV

Although it was the original intent of this reaction to form an tetrabutylammonium salt from the reaction of complex **I** and tetrabutylammonium hydroxide, after leaving the mixture standing at -25 °C the only product found were crystals of compound **IV**. After indexing these crystals' lattice, a search of the crystallographic data base found a corresponding structure, characterized by Kato *et al.* ¹⁵ as having a sodium ion as being the central atom connecting

asymmetrically to two bis(dithio-4-methylbenzoate) chelates. Upon refinement of our diffraction data this atom was actually determined to be a carbon atom as a methylene group. Another search of the crystallographic data base yielded similar structures^{10, 16} that were formed in a very similar manner to ours, via use of a counter cation source and usage of methylene chloride as a halogenated solvent. The NMR, MS and IR data acquired by those studies also fall very close to ours. The crystal parameters for our compound are displayed in Table 4, along with the crystal structure, Figure 3.

Given the novel synthesis of compound IV, another series of experiments were carried to generate similar compounds, $C(S_2CR)_n$, through use of other halogenated solvents. The results for these trials are shown in Table 3. It should be noted that this compound requires a phase-transfer process as just the presence of base is not enough to separate the perthio- ligands from the central zinc atom without substantial decomposition. Formation of this compound has also been achieved using tetramethylammonium hydroxide, though with a lower yield, 35%.

Table 3. Results of reactions for formation of compounds with formula C(S₂CR)_n.

Starting material	Solvent	Base	Solution color	Result ^b
$Zn(S_3CC_6H_5)_2$	CH ₂ Cl ₂	NBu ₄ OH	Deep red	Pink crystals
$Zn(S_3CC_6H_5)_2$	CH_2Cl_2	NMe ₄ OH	Deep red	Pink crystals
$Zn(S_3CC_6H_4CH_3)_2$	CH_2Cl_2	NMe ₄ OH	Deep red	Pink crystals
$Zn(S_3CC_6H_4CH_3)_2$	CHCl ₃	NBu ₄ OH	Brown-red	Ligand degradation
$Zn(S_3CC_6H_4CH_3)_2$	CHCl ₃	NaOH or KOH	Brown-red	Ligand degradation
$Zn(S_3CC_6H_4CH_3)_2$	CCl ₄	NBu ₄ OH	Brown-red	Ligand degradation

^aAll reaction conditions and methods are identical to those described in the experimental section for compound **IV**. ^bAll reaction mixtures were allowed to sit at -25 °C for 7 days before either crystals were collected or compound was characterized as having degraded.

Upon trying to form *tris*- or *tetra*- chelated complex using either chloroform or tetrachloromethane the perthio ligand underwent degradation under extended exposure to the solvents, indicating that the lability of those chloro groups is not as extensive as that found in methylene chloride or that there might be too much steric hindrance around the central carbon to allow so many dithio chelates to bind at once. Crystals of CH₂(S₂CC₆H₅)₂ were also grown by the same method using tetrabutylammonium hydroxide though at a lesser yield, 28%, suggesting that the presence of the methyl aromatic groups aids in allowing the compound to crystallize out of the organic solvent. These crystals were spectroscopically and analytically identical to those accidentally prepared by Liang *et al.*, ¹⁶ demonstrating that this procedure is a unique method for producing these class of compounds.

 Table 4. Crystallographic data for methylene bis(dithio-4-methylbenzoate).

Chemical formula	$C_{17}H_{14}S_4$
Formula weight/g mol ⁻¹	346.52
Crystal color and habit	pink rectangular prisms
Crystal size/mm	0.05 x 0.10 x 0.05
Crystal system	orthorhombic
Space group	P2 ₁ 2 ₁ 2
Unit cell dimensions	
a/Å	10.3646(11)
b/Å	18.7556(19)
c/Å	4.1148(4)
a (°)	90.00
β (°)	90.00
γ (°)	90.00
V/Å ³	799.89(14)
Z	2
T/K	100(2)
λ/Å	0.71073
Density _c (g cm ⁻¹)	1.439
$\mu(ext{Mo-K}lpha)/ ext{mm}^{-1}$	0.583
F(000)	360
Θ range (°)	2.17-28.51
No. reflections collected	9416
No. independent reflections	1938
Δ/σ_{max}	0.001
$I > 2\sigma(I)$	
R_I (obs. data)	0.0295
wR_2 (obs. data)	0.0822
wR_2 (all data)	0.0850
Goodness-of-fit on F^2 , S	0.634
Residual $\rho_{max}/e \mathring{A}^{-3}$	0.069

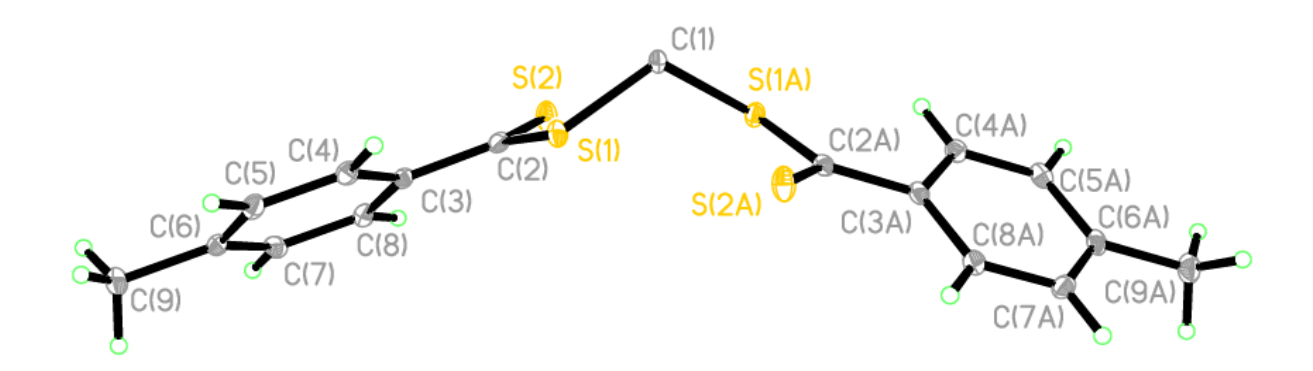


Figure 3. OTREP drawing of methylene bis(dithio-4-methylbenzoate).

Table 5. Selected bond distances (Å) and bond angles (°) for methylene bis(dithio-4-methylbenzoate).

(C1-S1	1.802(2)	C1-S1-C2	103.11(9)
S	S1-C2	1.747(3)	S1-C2-S2	123.13(15)
(C2-S2	1.644(3)	S1-C2-C3	113.25(19)
(C2-C3	1.482(3)	S2-C2-C3	123.6(2)
(C1-S1A	1.803(2)	S1-C1-S1A	118.4(2)

Table 5, above, shows some of the central bond angles of compound **IV**. The two-fold rotation axis with the central S-CH₂-S angle of 118.4° is significantly larger than the ideal tetrahedral value, possibly due to the electron repulsion between the two CS₂ groups. The C(2)-S(2) bond length of 1.644 Å is slightly longer than expected for a typical C=S double bond (\sim 1.61 Å)¹⁶ while the C(1)-S(1) bond length of 1.802 Å is long enough to be clearly identified as a single bond, and on par with those reported by Shrivastav *et al.*¹⁰ Though the structure of the compound plainly shows that its chelates' geometry is no longer square-planar like its parent complex, in comparison to the findings of Bonamico *et al.*¹⁷ the bond angles are very similar,

bending about 103° around S1 at a C1-S1 bond length of ~ 1.7 Å. In correspondence with the data of the original structure produced by Kato, ¹⁸ the dihedral angle of the phenyl ring is out of the plane for the CS₂ group attached to it, possibly allowing for some delocalization of the negative charge on the dithiocarboxyl group.

The density functional theory (DFT) gas phase structure was also calculated for compound **IV** (Figure 4). As can be viewed on Table 6 the differences between the theoretical values for its structure and the actual values determined vary by as much as 0.03 Å per bond length and 8° per bond angle. While this divergence might not be considered significantly large it is very telling as to the nature of the bonds within this molecule. It is distinguishing that the phase structure model is at least somewhat on par with the values found for the crystal structure of compound **IV**, if not exact. Compared to the theoretical values, it can seem that all the bonds for methylene bis(dithio-4-methylbenzoate) are smaller, and therefore stronger, and the repulsion between the thiocarbonyl sulfur lone pairs more influential, indicated by the larger than expected value for the S-CH₂-S angle.

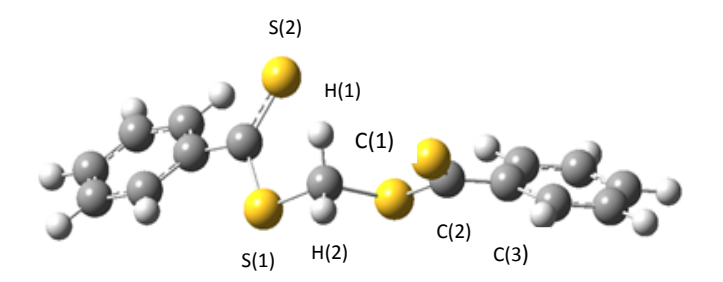


Figure 4. Gas phase structure of compound **IV**, where both aromatic rings are below the S-CH₂-S plane.

Table 6. Comparison of selected theoretical (B3LYP/6-3Htt6xx) gas phase structure and crystal structure of compound **IV**.

Theoretical b	ond length	ΔÅ	Theoretical bond angle	Δ^{o}
C(1)-S(1)	1.81345	0.01125	S(1)-C(1)-S(1A) 110.29764	-8.12236 ^c
S(1)-C(2)	1.77928	0.03198	C(1)-S(1)-C(2) 102.5617	-0.5573
C(2)-S(2)	1.65066	0.00636	S(1)-C(2)-S(2) 124.296	1.1645
C(1)-S(1A)	1.76397	0.02889	S(2)-C(2)-C(3) 123.43	-0.19
$S(1)-H(1)^a$	2.65572		S(1)-C(2)-C(3) 112.263	-0.9889
$C(1)$ - $H(1)^b$	1.08866			

^aS(1)-H(1) corresponds to a hydrogen bond between a methylene proton and a lone pair on a thiocarbonyl sulfur. ^bThis value was not calculated for Figure 3 but the theoretical value is typical for C-H bonds. ^cNegative values are due to the corresponding theoretical value being smaller than the one actually determined.

4.5. Conclusions

Sulfur-rich ligands offer a diverse range of chemical reactions, from the ability to reversibly elimination or abstract sulfur¹⁰ to substitution onto a halogenated solvent. As versatile sulfur-derivatives they have considerable potential as substrates for carbon-carbon bond formations and may display biological activity.¹⁹ The formation of dimerized molecules such as compound **IV** from transition metal-coordinated chelates is not uncommon ^{15,16} and might usually require a metal-assisted transformation.²⁰⁻²² These compounds appear to be fairly robust as well and only begin to decompose under harsher conditions such as high temperatures or basic environments. Further study needs to be undertaken to examine the extent of these ligands' reactivity with focus on structural analysis as a mode of determining the relative strengths of their intramolecular bonds.

4.6. References

- 1. Mas-Balleste, R.; Guijarro, A.; Gonzalez-Prieto, R.; Castillo, O.; Sanz Miguel, P.J.; Zamora,
- F. S-S bond reactivity in metal-perthiocarboxylato compounds *Dalton Trans.*, **2010**, *39(6)*, 1511.
- 2. Petersen, B.M.; Bjernemose, J.K.; Jeppesen, J.O. Characterization of a byproduct in the alkylation of DMIT: Alkylation on the least nucleophilic sulfur atom *Eur. J. Inorg. Chem.*, **2006**, *15*, 3099.
- 3. Coucouvanis, D.; Fackler Jr., J.P. Sulfur chelates. IV. Sulfur addition to dithiolato complexes of Ni^(II). *J. Amer. Chem. Soc.*, **1967**, *89(6)*, 1346.
- 4. Fackler Jr., J.P.; Fetchin, J.A.; Fries, D.C.; Sulfur chelates. XV. Sulfur addition and abstraction reactions of dithioaryl acid complexes of Zn^(II), Ni^(II), Pd^(II) and Pt^(II). *J. Amer. Chem. Soc.*, **1972**, *94*(7), 7323.
- 5. Wilberg, N.; Holleman, A.F.; Wilberg, E. *Inorganic Chemistry*. Academic Press, **2001**, 521.
- 6. Fackler Jr., J.P.; Coucouvanis, D.; Fetchin, J.A.; Seidel, W.C. Sulfur chelates. VIII. Oxidative addition to sulfur to dithioaryl acid complexes of Ni^(II) and Zn^(II). *J. Amer. Chem. Soc.*, **1968**, *90(11)*, 2784.
- 7. Bruni, G.; Levi, T.G. A method for the preparation of organo dithio acids. *Atti Accad. Lincei.*, **1923**, *32*, 5.
- 8. Camus, A.; Marisch, N. On some Cu⁽¹⁾ perthiocarboxylates and their reactions with tertiary phosphines. *Inorg. Chim. Acta*, **1989**, *161(1)*, 87.

- 9. Shrivastav, A.; Singh, N.K.; Srivastava, G. Synthesis, characterization and antitumor studies of transition metal complexes of o-hydroxydithiobenzoate. *Bioorg. Med. Chem.* **2002**, *10(8)*, 2693.; Shrivastav, A.; Singh, N.K.; Singh, S.M. Synthesis, characterization and antitumor studies on Mn^(II), Fe^(II), Co^(II), Ni^(II), Cu^(II) and Zn^(II) complexes of o-hydroxydithiobenzoate. *Bioorg. Med. Chem.* **2002**, *10(8)*, 2693.
- 10. Fackler Jr., J.P.; Fetchin, J.A.; Smith, J.A. Sulfur chelates. X. Sulfur addition and abstraction in Ni^(II) and Zn^(II) dithiobenzoates. *J. Amer. Chem. Soc.*, **1970**, *92*(*9*), 2910.; Fackler Jr., J.P.; Fetchin, J.A. Sulfur chelates. XI. Sulfur ability in sulfur-rich metal dithiolates. *J. Amer. Chem. Soc.*, **1970**, *92*(*9*), 2912.
- 11. Kato, S.; Shibahashi, H.; Katada, T.; Takagi, T.; Noda, I.; Mizuta, M.; Goto, M. Preparation and some reactions bis(thioacyl) sulfides. *Liebigs Ann. Chem.*, **7**, 1229 (1982)
- 12. Buadron, S.A.; Hossein, M.W.; Kyritsakas, N.; Kurmoo, M. A step-wise approach to the formation of heterometallic discrete complexes and infinite architectures. *Dalton Trans.*, **2007**, 1129.
- 13. Bereman, R.D.; Nalewajek, D. Ni^(II), Pd^(II), and Pt^(II) complexes of the dithiolate ligand, C₅H₄CS₂²⁻. *Inorg. Chem.*, **1976**, *15*(*12*), 2981.
- 14. Pellizier, G.; Marisch, N.; Camus, A. Structural features of Cu⁽¹⁾ perthio- and dithiocarboxyalates from carbon-13 NMR spectra. *Inorg. Chim. Acta*, **1989**, *155*(2), 167.
- 15. Kato, S.; Ito, K.; Hattori, R.; Mizuta, M.; Kateda, T. A simple method for the preparation of anhydrous sodium dithiocarboxylates. *Naturforsch.*, **1978**, *33B(9)*, 976.

- 16. Liang, Y.-R.; Tong, H.-C.; Lo, Y.-H.; Lin, C.-H.; Kuo, T.S. Methylenebis(dithobenzoate). *Acta Cryst. E.*, 2008, *64(12)*, o2366.
- 17. Bonamico, M.; Dessy, G.; Fares, V.; Scaramuzza, L. Crystal structure of bis(dithiobenzoato)zinc^(II). *J. Chem. Soc. Dalton Trans.*, **1972**, *22*, 2515.
- 18. Kato, S.; Kitaoka, N.; Niyomura, O.; Kitoh, Y.; Kanda, T.; Ebihara, M. Heavy alkali metal arenedithiocarboxylates. *Inorg. Chem.*, **1999**, *38(3)*, 496.
- 19. Gonzalez-Castro, A.; Gutierrez-Perez, R.; Peneries-Carrillo, G.; Diaz-Torres, E.; Toscano, R.A.; Moya-Cabrera, M.; Cabrera-Ortiz, A.; Alvarez-Toledano, C. A straightforward and novel synthesis of sulfur compounds from aliphatic cyclic ketones and CS₂. *Heteroatom Chem.*, **2000**, *11(2)*, 120.
- 20. Nakayama, J.; Akiyama, I. Unexpected formation of an inner salt, bis(N,N-diethylamino)carbenium dithiocarboxylate, from 2-chloro or 2-phenoxy substituted 1,1-bis(N.N-diethylamino)ethylenes and elemental sulfur. *J. Chem. Soc. Comm.*, **1992**, *20*, 1552.
- 21. Nakayama, J. Kitahara, T.; Sugihara, Y.; Sakamoto, Y. Isolable, stable diselenocarboxylate and selenothiocaboxylate salts, *J. Am. Chem. Soc.*, **2000**, *122(38)*, 9120.
- 22. Banerjee, S.R.; Zubieta, J. A metal-mediated dimerization of the ligand bis(*N*, *N*-diethylamino)-carbeniumdithiocarboxylate. *Acta Crsyt.*, **2004**, *C60*, 208.

CONCLUSIONS AND FUTURE WORK

Considerable interest has risen in recent years in studying transition metal thiolates and other sulfur derivatives due to their use in biological, synthetic and environmental applications. There has been much precedence for the theory that sulfur groups become potent nucleophiles once coordinated to metal centers that allow for two-electron oxidation, and our current study focuses on generating such complexes, particularly stable, four- to six-coordinate complexes which still exhibit high reactivity. Many of these types of complexes have the ability to reversible bind other small molecules through oxidative addition though the reactivity of these complexes bear a strong ligand-dependence. Sulfur-rich complexes, specifically those of sulfur chelates, also have the ability to undergo oxidation to yield disulfides and tend to be more relatively stable then other oxygenated-derivatives, allowing for better analysis of organic compounds. Recently, there has been many cases of sulfur-containing heterocycles being able to reversibly add and eliminate sulfur atoms, permitting better investigation into the dynamics of the ring-opening mechanism as well as the kinetic dynamics that drive such reactions. Due to the continually growing trends in examining sulfur-containing complexes, it was the purpose of this study to investigate the coordination spheres of these types of complexes as well as analyze the reactivity of some of these thiol groups by transition metal alpha effects.

In Chapter Two, it was seen that d⁶ iridium complexes are not as kinetically stable as expected and that the thiolates of the metal centers are quite labile, undergoing reductive elimination and substitution under ambient conditions. The hydrides added to these complexes upon *cis* or *trans* oxidative addition seem to be retained more readily than the thiols, possibly indicating that the sulfur groups are made more reactive by the presence of the metal. This

lability might also present a pathway to build more complex biomimetic models by taking advantage of this property to insure the coordination of other, more favorable ligands.

Chapter Three explored the possibility of generating similar d⁸ to d⁶ iridium compounds in order to examine the differences in their respective reactivity. It was found that while some of these compounds do react with thiols, their structures, due to the possibility of dimerization, are harder to resolve as a result of similar elemental composition and low solubility in most organic solvents. While the innate insolubility of these class of compounds is highly indicative of possible dimer formation, several of these iridium-thiol compounds, including those in Chapter Two, have been found to consist of many isomers upon coordination of even the weakest acidic molecules. It has been found by this study, as well as several others, that this phenomena is in part due to solvent effects, where there is a shift in equilibrium between these isomers, but other factors have yet to still be further investigated.

The sulfur-rich ligands of Chapter Four offer a diverse range of potential reactions, from the ability to reversibly elimination or abstract sulfur, substitute onto a di-halogenated solvent or even substituted onto different metallic centers. Due to the versatility of these sulfur-derivatives, they have great potential as substrates as many of them do exhibit biological activity. These compounds can even be used to form robust dimerized molecules from reactions with halogenated solvents through metal-assisted transformations in quantitative yields and with tunable UV/visible properties. The mechanism for these types of substitution reactions has yet to be fully explored can open doors to forming other similar compounds with other halogenated solvents besides dichloromethane.

Proposed future work would include further attempts to substitute other ligands onto complex **I** of Chapter Two in order to decrease the apparent lability of its sulfhydryl group. Once this goal could be achieved, it would be novel to examine the enhanced nucleophilicity on this group toward electrophiles compared to that of the free ligand, HS⁻, alone. Considering that the thiolate groups of the complexes in this chapter are quite labile ligands, it would be interesting to evaluate whether or not these groups can be substituted onto other electrophiles as well.

Another route could be further exploring the reactions of the [Ir(dppe)₂]Cl systems from Chapter Three with bulkier aromatic thiols in order to see if they would still bind despite the steric hindrance of the diphenyl phosphine chelates on the complex. More NMR experiments and crystallization efforts on complexes III-V are also required in order to resolve their actual structures as well, and building a library of more thiol reactions with the dinitrogen analogue of Vaska's compound would be useful in order to determine the unique complexes that can be produced.

Lastly, it would also be worthwhile to study the reactions of the zinc perthio chelates of Chapter Four with other chlorinated transition metal compounds such as IrCl₃, FeCl₃ or RuCl₃ since it has been found to react with CoCl₂, PtCl₂, PtCl₄ and PdCl₂. Further attempts to substitute the perthio and dithio bidentate ligands onto other metal complexes should be made as well in the hopes of forming equally diverse trigonal bipyramidal or octahedral compounds with these complexes.

ACKNOWLEDGEMENTS

I would like to take the time to acknowledge all the members of the Bohle research group at McGill University for their contributions to this study, including Kristopher Rosadiuk, Dr. Ivor Wharf, Dr. Zhijie Chua, Joel Poisson and Alexander Waked. A special thanks goes out to Dr. D. Scott Bohle for his help in resolving every crystal structure found in this thesis and for his input on the projects that allowed me to complete this study. I would like to acknowledge Dr. Alexander Wahba and Dr. Fred Morin for their assistance and expertise in analyzing mass spectra and NMR data, respectively. I would also like to the thank several foundations for their generous funding of my work, not limited to the Natural Sciences and Engineering Research Council of Canada and Canada Research Chairs program. Lastly I would like to thank my family and the academic coordinators in the graduate chemistry department of McGill University for all their help in making this thesis a reality. Thank you all sincerely.

FINAL FANTASY MMXV



THANK YOU FOR READING!

NEN GAME Load game Gradvate

APPENDIX

Complex II from Chapter Two

 $\textbf{Table 1.} \ Fractional \ atomic \ coordinates \ and \ isotropic \ or \ equivalent \ isotropic \ displacement \ parameters \ (\mathring{A}^2)$

	X	у	Z	$U_{ m iso}$ */ $U_{ m eq}$
Ir	0.80485 (3)	0.092093 (15)	0.285102 (19)	0.03972 (13)
Cl	0.60817 (19)	0.02130 (10)	0.26369 (12)	0.0431 (5)
I	0.69693 (7)	0.19306 (3)	0.20542 (4)	0.0633 (2)
C1	0.9598 (11)	0.1338 (5)	0.3094 (6)	0.059 (2)
O1	1.0556 (7)	0.1597 (5)	0.3251 (5)	0.098 (3)
P1	0.7300 (2)	0.12144 (10)	0.40680 (14)	0.0426 (5)
C10	0.7248 (10)	0.0598 (4)	0.4784 (6)	0.054 (2)
C11	0.798 (2)	0.0109 (8)	0.4757 (10)	0.162 (10)
H11A	0.8485	0.0048	0.4337	0.195*
C12	0.800 (3)	-0.0330 (9)	0.5377 (13)	0.174 (11)
H12A	0.8551	-0.0665	0.5356	0.209*
C13	0.7306 (15)	-0.0290 (7)	0.5955 (9)	0.092 (4)
H13A	0.7372	-0.0563	0.6373	0.111*
C14	0.652 (2)	0.0149 (12)	0.5911 (15)	0.209 (15)
H14A	0.5923	0.0172	0.6287	0.251*
C15	0.648 (2)	0.0599 (10)	0.5348 (13)	0.170 (11)
H15A	0.5888	0.0916	0.5375	0.204*
C20	0.5735 (9)	0.1612 (4)	0.4064 (6)	0.049 (2)
C21	0.5501 (12)	0.1990 (5)	0.4686 (7)	0.072 (3)
H21A	0.6142	0.2034	0.5107	0.086*
C22	0.4315 (11)	0.2305 (6)	0.4693 (8)	0.076 (3)
H22A	0.4173	0.2559	0.5113	0.091*

C23	0.3378 (11)	0.2240 (6)	0.4086 (8)	0.077 (3)
H23A	0.2585	0.2447	0.4089	0.093*
C24	0.3592 (10)	0.1871 (5)	0.3469 (7)	0.069 (3)
H24A	0.2945	0.1833	0.3051	0.082*
C25	0.4771 (9)	0.1547 (5)	0.3454 (6)	0.060(3)
H25A	0.4898	0.1290	0.3033	0.072*
C30	0.8450 (9)	0.1769 (4)	0.4542 (5)	0.048 (2)
C31	0.9351 (12)	0.1640 (6)	0.5175 (7)	0.074 (3)
H31A	0.9361	0.1257	0.5407	0.089*
C32	1.0225 (15)	0.2072 (7)	0.5460 (8)	0.101 (5)
H32A	1.0812	0.1983	0.5895	0.121*
C33	1.0255 (13)	0.2632 (6)	0.5121 (8)	0.084 (4)
Н33А	1.0878	0.2918	0.5308	0.100*
C34	0.9348 (12)	0.2767 (5)	0.4496 (7)	0.076 (3)
H34A	0.9338	0.3150	0.4265	0.091*
C35	0.8476 (11)	0.2341 (5)	0.4223 (7)	0.066 (3)
H35A	0.7868	0.2438	0.3802	0.079*
P2	0.8821 (2)	0.05317 (10)	0.16824 (14)	0.0433 (5)
C40	1.0454 (9)	0.0824 (4)	0.1532 (6)	0.051 (2)
C41	1.0589 (10)	0.1443 (5)	0.1413 (6)	0.065 (3)
H41A	0.9858	0.1696	0.1395	0.078*
C42	1.1821 (12)	0.1684 (6)	0.1322 (7)	0.078 (4)
H42A	1.1914	0.2100	0.1248	0.094*
C43	1.2904 (12)	0.1312 (8)	0.1339 (8)	0.086 (4)
H43A	1.3721	0.1472	0.1257	0.103*
C44	1.2774 (12)	0.0718 (9)	0.1475 (10)	0.108 (5)
H44A	1.3515	0.0471	0.1511	0.130*
C45	1.1554 (10)	0.0461 (6)	0.1564 (8)	0.078 (3)

H45A	1.1482	0.0044	0.1646	0.093*
C50	0.7866 (9)	0.0690 (4)	0.0739 (5)	0.049 (2)
C51	0.8468 (11)	0.0849 (5)	0.0077 (6)	0.064 (3)
H51A	0.9377	0.0889	0.0108	0.077*
C52	0.7716 (15)	0.0949 (6)	-0.0637 (7)	0.082 (4)
H52A	0.8122	0.1071	-0.1077	0.099*
C53	0.6387 (14)	0.0870 (5)	-0.0694 (7)	0.073 (3)
H53A	0.5898	0.0922	-0.1177	0.088*
C54	0.5767 (11)	0.0715 (5)	-0.0047 (7)	0.070(3)
H54A	0.4859	0.0670	-0.0087	0.084*
C55	0.6504 (10)	0.0625 (5)	0.0675 (6)	0.059 (2)
H55A	0.6083	0.0521	0.1117	0.071*
C60	0.8989 (9)	-0.0296 (4)	0.1693 (6)	0.052 (2)
C61	0.9591 (13)	-0.0580 (6)	0.2364 (7)	0.078 (3)
H61A	0.9919	-0.0352	0.2798	0.094*
C62	0.9690 (16)	-0.1210 (6)	0.2369 (9)	0.092 (4)
H62A	1.0040	-0.1404	0.2826	0.111*
C63	0.9285 (13)	-0.1554 (5)	0.1716 (9)	0.085 (4)
H63A	0.9418	-0.1972	0.1722	0.102*
C64	0.8708 (13)	-0.1288 (5)	0.1082 (9)	0.077 (3)
H64A	0.8389	-0.1521	0.0650	0.093*
C65	0.8577 (10)	-0.0654 (5)	0.1059 (7)	0.061 (3)
H65A	0.8200	-0.0471	0.0601	0.073*
C47	0.3977 (19)	0.1412 (9)	-0.2727 (11)	0.123 (6)
H47A	0.3970	0.1022	-0.2462	0.147*
H47B	0.3413	0.1693	-0.2477	0.147*
C12	0.5732 (19)	0.1726 (5)	-0.2719 (6)	0.335 (8)
C13	0.3491 (11)	0.1340 (6)	-0.3733 (7)	0.293 (6)

Table 2. Atomic displacement parameters (\mathring{A}^2)

	U^{11}	U^{22}	U^{33}	U^{12}	U^{13}	U^{23}
Ir	0.03310 (19)	0.04014 (19)	0.0458 (2)	-0.00013 (13)	0.00325 (13)	0.00060 (13)
Cl	0.0338 (10)	0.0559 (12)	0.0409 (10)	-0.0042 (8)	0.0093 (8)	-0.0047 (8)
I	0.0678 (5)	0.0546 (4)	0.0658 (4)	0.0072 (3)	-0.0016 (3)	0.0060(3)
C1	0.063 (6)	0.066 (6)	0.049 (5)	0.002 (5)	0.014 (5)	-0.004 (5)
O1	0.045 (4)	0.147 (9)	0.101 (7)	-0.038 (5)	0.007 (4)	-0.039 (6)
P1	0.0386 (11)	0.0415 (11)	0.0477 (13)	-0.0002 (9)	0.0043 (9)	-0.0014 (9)
C10	0.049 (5)	0.052 (5)	0.059 (6)	-0.007 (4)	0.007 (4)	0.009 (4)
C11	0.27 (3)	0.113 (13)	0.119 (13)	0.121 (15)	0.113 (15)	0.065 (11)
C12	0.27 (3)	0.114 (14)	0.149 (17)	0.107 (17)	0.081 (19)	0.071 (13)
C13	0.096 (10)	0.092 (10)	0.090 (10)	-0.005 (8)	0.011 (8)	0.043 (8)
C14	0.20(2)	0.23 (3)	0.22(3)	0.11 (2)	0.14(2)	0.16(2)
C15	0.175 (19)	0.164 (18)	0.19(2)	0.100 (16)	0.131 (17)	0.118 (16)
C20	0.042 (5)	0.044 (5)	0.062 (6)	0.000 (4)	0.008 (4)	0.000 (4)
C21	0.072 (7)	0.074 (7)	0.067 (7)	0.010 (6)	-0.005 (6)	-0.023 (6)
C22	0.059 (7)	0.078 (8)	0.093 (9)	0.017 (6)	0.018 (6)	-0.028 (6)
C23	0.050 (6)	0.072 (7)	0.112 (10)	0.011 (5)	0.019 (6)	-0.009 (7)
C24	0.038 (5)	0.080(8)	0.089(8)	0.004 (5)	0.009 (5)	-0.007 (6)
C25	0.041 (5)	0.067 (6)	0.072 (7)	0.002 (5)	0.003 (5)	-0.008 (5)
C30	0.041 (5)	0.052 (5)	0.050 (5)	-0.005 (4)	-0.001 (4)	-0.004 (4)
C31	0.087 (8)	0.067 (7)	0.068 (7)	-0.007 (6)	-0.004 (6)	0.002 (5)
C32	0.105 (11)	0.101 (10)	0.086 (9)	-0.029 (9)	-0.040 (8)	-0.002 (8)
C33	0.080 (9)	0.087 (9)	0.081 (8)	-0.036 (7)	-0.005 (7)	-0.014 (7)
C34	0.089 (9)	0.055 (6)	0.083 (8)	-0.025 (6)	-0.001 (7)	-0.001 (5)
C35	0.069 (7)	0.056 (6)	0.069 (7)	-0.013 (5)	-0.011 (5)	-0.001 (5)
P2	0.0357 (11)	0.0446 (11)	0.0497 (13)	0.0017 (9)	0.0049 (9)	0.0002 (9)
C40	0.039 (5)	0.062 (6)	0.050 (5)	0.001 (4)	0.004 (4)	-0.003 (4)

C41	0.050(6)	0.078 (7)	0.068 (7)	-0.006 (5)	0.008 (5)	0.016 (5)
C42	0.072 (8)	0.094 (9)	0.068 (7)	-0.034 (7)	0.007 (6)	0.015 (6)
C43	0.054 (7)	0.120 (12)	0.086 (9)	-0.029 (8)	0.017 (6)	-0.018 (8)
C44	0.041 (7)	0.130 (14)	0.155 (15)	0.000(8)	0.014 (8)	-0.026 (12)
C45	0.042 (6)	0.073 (7)	0.120 (10)	0.003 (5)	0.019 (6)	-0.004 (7)
C50	0.052 (5)	0.046 (5)	0.050 (5)	0.007 (4)	0.002 (4)	-0.002 (4)
C51	0.059 (6)	0.078 (7)	0.056 (6)	0.002 (5)	0.005 (5)	0.001 (5)
C52	0.096 (10)	0.100 (10)	0.052 (7)	0.008 (7)	0.010 (6)	0.003 (6)
C53	0.091 (9)	0.071 (7)	0.053 (6)	0.014 (6)	-0.017 (6)	-0.003 (5)
C54	0.052 (6)	0.076 (7)	0.078 (8)	0.004 (5)	-0.015 (6)	-0.004 (6)
C55	0.053 (6)	0.062 (6)	0.062 (6)	0.000 (5)	0.002 (5)	0.007 (5)
C60	0.044 (5)	0.046 (5)	0.068 (6)	0.007 (4)	0.013 (4)	0.004 (4)
C61	0.102 (10)	0.068 (7)	0.066 (7)	0.028 (7)	0.010 (6)	0.008 (6)
C62	0.133 (13)	0.062 (7)	0.084 (9)	0.030 (8)	0.024 (9)	0.014 (7)
C63	0.092 (9)	0.041 (6)	0.127 (12)	0.005 (6)	0.041 (9)	0.008 (7)
C64	0.083 (8)	0.050 (6)	0.102 (10)	0.003 (6)	0.024 (7)	-0.008 (6)
C65	0.062 (6)	0.050 (5)	0.072 (7)	-0.001 (5)	0.013 (5)	-0.005 (5)
C47	0.141 (16)	0.122 (14)	0.109 (14)	0.020 (12)	0.030 (12)	-0.001 (11)
C12	0.60(3)	0.207 (10)	0.189 (9)	-0.035 (13)	-0.004 (12)	0.037 (7)
C13	0.265 (11)	0.383 (15)	0.234 (11)	0.150 (11)	0.039 (9)	0.083 (10)

Table 3. Geometric parameters (Å, $^{\rm o}$)

Ir—C1	1.844 (11)	C33—C34	1.377 (17)
Ir—P1	2.367 (2)	C34—C35	1.346 (14)
Ir—P2	2.371 (2)	P2—C60	1.828 (9)
Ir—Cl	2.543 (2)	P2—C40	1.829 (10)
Ir—I	2.7772 (7)	P2—C50	1.835 (9)
C1—O1	1.143 (12)	C40—C45	1.377 (14)

D1 C20	1 922 (0)	C40 C41	1 205 (15)
P1—C20	1.823 (9)	C40—C41	1.385 (15)
P1—C30	1.829 (9)	C41—C42	1.389 (15)
P1—C10	1.829 (10)	C42—C43	1.376 (19)
C10—C15	1.294 (18)	C43—C44	1.33 (2)
C10—C11	1.314 (16)	C44—C45	1.391 (17)
C11—C12	1.43 (2)	C50—C51	1.379 (14)
C12—C13	1.27 (2)	C50—C55	1.394 (13)
C13—C14	1.25 (2)	C51—C52	1.396 (16)
C14—C15	1.38 (2)	C52—C53	1.365 (19)
C20—C25	1.372 (13)	C53—C54	1.364 (17)
C20—C21	1.386 (13)	C54—C55	1.396 (14)
C21—C22	1.398 (15)	C60—C65	1.372 (14)
C22—C23	1.350 (16)	C60—C61	1.394 (14)
C23—C24	1.362 (16)	C61—C62	1.390 (17)
C24—C25	1.403 (14)	C62—C63	1.377 (19)
C30—C35	1.371 (14)	C63—C64	1.319 (18)
C30—C31	1.381 (14)	C64—C65	1.401 (15)
C31—C32	1.363 (16)	C47—C13	1.75 (2)
C32—C33	1.363 (19)	C47—C12	1.92 (2)
C1—Ir—P1	90.5 (3)	C32—C31—C30	120.1 (11)
C1—Ir—P2	91.2 (3)	C33—C32—C31	121.3 (12)
P1—Ir—P2	174.52 (8)	C32—C33—C34	118.8 (10)
C1—Ir—Cl	171.2 (3)	C35—C34—C33	119.6 (11)
P1—Ir—Cl	88.66 (7)	C34—C35—C30	122.5 (10)
P2—Ir—Cl	88.83 (7)	C60—P2—C40	105.4 (4)
C1—Ir—I	90.3 (3)	C60—P2—C50	103.9 (4)
P1—Ir—I	93.68 (6)	C40—P2—C50	103.2 (4)
P2—Ir—I	91.51 (6)	C60—P2—Ir	112.9 (3)

Cl—Ir—I	98.44 (5)	C40—P2—Ir	111.8 (3)
O1—C1—Ir	179.5 (10)	C50—P2—Ir	118.4 (3)
C20—P1—C30	102.1 (4)	C45—C40—C41	118.9 (10)
C20—P1—C10	106.1 (4)	C45—C40—P2	123.0 (8)
C30—P1—C10	104.9 (4)	C41—C40—P2	118.1 (7)
C20—P1—Ir	118.9 (3)	C40—C41—C42	119.7 (11)
C30—P1—Ir	108.8 (3)	C43—C42—C41	120.5 (12)
C10—P1—Ir	114.5 (3)	C44—C43—C42	119.5 (11)
C15—C10—C11	114.4 (12)	C43—C44—C45	121.5 (13)
C15—C10—P1	123.5 (10)	C40—C45—C44	119.8 (13)
C11—C10—P1	122.1 (10)	C51—C50—C55	118.8 (9)
C10—C11—C12	119.6 (15)	C51—C50—P2	121.5 (8)
C13—C12—C11	123.9 (16)	C55—C50—P2	119.7 (7)
C14—C13—C12	114.0 (15)	C50—C51—C52	120.1 (11)
C13—C14—C15	125.0 (18)	C53—C52—C51	120.3 (12)
C10—C15—C14	122.4 (16)	C52—C53—C54	120.6 (11)
C25—C20—C21	118.7 (9)	C53—C54—C55	119.6 (11)
C25—C20—P1	121.4 (7)	C50—C55—C54	120.5 (10)
C21—C20—P1	120.0 (8)	C65—C60—C61	117.9 (10)
C20—C21—C22	121.0 (10)	C65—C60—P2	122.9 (8)
C23—C22—C21	119.7 (10)	C61—C60—P2	119.2 (8)
C22—C23—C24	120.0 (10)	C62—C61—C60	118.6 (12)
C23—C24—C25	121.2 (11)	C63—C62—C61	121.7 (12)
C20—C25—C24	119.3 (10)	C64—C63—C62	119.8 (11)
C35—C30—C31	117.6 (9)	C63—C64—C65	119.8 (12)
C35—C30—P1	118.1 (7)	C60—C65—C64	122.0 (11)
C31—C30—P1	124.2 (8)	C13—C47—C12	102.7 (11)

Complex III from Chapter Two

Table 4. Fractional atomic coordinates and isotropic or equivalent isotropic displacement parameters (\mathring{A}^2)

	x	У	Z	$U_{ m iso}$ */ $U_{ m eq}$
Ir	0.249333 (5)	0.113759 (5)	0.195381 (4)	0.01175 (3)
Cl	0.41149 (3)	0.11230 (3)	0.31406 (3)	0.01630 (9)
C1	0.29181 (14)	0.06907 (13)	0.11771 (12)	0.0155 (4)
O	0.31080 (11)	0.04398 (10)	0.06605 (10)	0.0236 (3)
S	0.17223 (4)	0.17071 (3)	0.27923 (3)	0.01754 (10)
P1	0.21482 (3)	-0.02683 (3)	0.23427 (3)	0.01354 (9)
P2	0.27378 (3)	0.25916 (3)	0.16206 (3)	0.01317 (9)
C2	0.04488 (15)	0.16294 (14)	0.22153 (14)	0.0216 (4)
C3	-0.00910 (17)	0.13214 (15)	0.26293 (16)	0.0274 (5)
Н3А	0.0230	0.1118	0.3187	0.033*
C4	-0.10825 (19)	0.13075 (17)	0.22424 (18)	0.0336 (6)
H4A	-0.1429	0.1087	0.2537	0.040*
C5	-0.15829 (17)	0.16127 (18)	0.14245 (19)	0.0355 (6)
C6	-0.10439 (16)	0.19175 (16)	0.10270 (16)	0.0287 (5)
H6A	-0.1367	0.2129	0.0472	0.034*
C7	-0.00520 (16)	0.19308 (15)	0.13991 (15)	0.0257 (5)
H7A	0.0289	0.2146	0.1098	0.031*
C8	-0.2664 (2)	0.1617 (3)	0.0998 (2)	0.0568 (9)
H8A	-0.2876	0.1850	0.0431	0.085*
H8B	-0.2915	0.1987	0.1314	0.085*
H8C	-0.2904	0.1016	0.0972	0.085*
C11	0.27082 (15)	-0.11809 (13)	0.20366 (13)	0.0180 (4)
C12	0.22456 (18)	-0.19888 (16)	0.17943 (19)	0.0363 (6)

H12A	0.1636	-0.2075	0.1797	0.044*
C13	0.26765 (19)	-0.26703 (18)	0.1549 (2)	0.0452 (8)
H13A	0.2363	-0.3222	0.1395	0.054*
C14	0.35568 (17)	-0.25478 (17)	0.15275 (17)	0.0331 (6)
H14A	0.3837	-0.3006	0.1340	0.040*
C15	0.40260 (16)	-0.17524 (15)	0.17818 (14)	0.0244 (5)
H15A	0.4635	-0.1668	0.1777	0.029*
C16	0.36114 (15)	-0.10760 (13)	0.20435 (14)	0.0194 (4)
H16A	0.3946	-0.0538	0.2229	0.023*
C21	0.25793 (15)	-0.03889 (13)	0.34719 (12)	0.0170 (4)
C22	0.19980 (16)	-0.01546 (14)	0.38720 (14)	0.0213 (4)
H22A	0.1357	0.0029	0.3551	0.026*
C23	0.23553 (19)	-0.01895 (15)	0.47374 (14)	0.0274 (5)
H23A	0.1954	-0.0044	0.5006	0.033*
C24	0.3298 (2)	-0.04374 (15)	0.52064 (14)	0.0305 (5)
H24A	0.3544	-0.0457	0.5797	0.037*
C25	0.38822 (18)	-0.06567 (15)	0.48187 (14)	0.0283 (5)
H25A	0.4530	-0.0818	0.5145	0.034*
C26	0.35257 (16)	-0.06434 (14)	0.39520 (13)	0.0226 (4)
H26A	0.3926	-0.0807	0.3688	0.027*
C31	0.08754 (14)	-0.05524 (13)	0.19066 (13)	0.0156 (4)
C32	0.05067 (16)	-0.11347 (13)	0.23130 (14)	0.0211 (4)
H32A	0.0925	-0.1407	0.2820	0.025*
C33	-0.04735 (16)	-0.13148 (14)	0.19741 (15)	0.0237 (5)
Н33А	-0.0721	-0.1706	0.2254	0.028*
C34	-0.10894 (16)	-0.09258 (15)	0.12315 (15)	0.0237 (5)
H34A	-0.1758	-0.1041	0.1009	0.028*
C35	-0.07274 (15)	-0.03696 (15)	0.08151 (14)	0.0224 (4)

H35A	-0.1146	-0.0115	0.0299	0.027*
C36	0.02493 (15)	-0.01826 (14)	0.11516 (13)	0.0186 (4)
H36A	0.0492	0.0202	0.0863	0.022*
C41	0.16160 (14)	0.31098 (13)	0.09416 (13)	0.0170 (4)
C42	0.10867 (16)	0.27539 (15)	0.01496 (13)	0.0220 (4)
H42A	0.1349	0.2292	-0.0050	0.026*
C43	0.01756 (17)	0.30761 (17)	-0.03470 (15)	0.0303 (5)
H43A	-0.0179	0.2839	-0.0888	0.036*
C44	-0.02141 (18)	0.37407 (18)	-0.00537 (17)	0.0356 (6)
H44A	-0.0839	0.3954	-0.0392	0.043*
C45	0.03036 (18)	0.40968 (17)	0.07317 (17)	0.0323 (5)
H45A	0.0032	0.4552	0.0931	0.039*
C46	0.12207 (16)	0.37874 (14)	0.12288 (14)	0.0225 (4)
H46A	0.1578	0.4037	0.1764	0.027*
C51	0.33161 (14)	0.34241 (13)	0.24268 (12)	0.0162 (4)
C52	0.36490 (17)	0.41878 (14)	0.21919 (14)	0.0232 (4)
H52A	0.3580	0.4250	0.1635	0.028*
C53	0.40779 (18)	0.48537 (15)	0.27642 (15)	0.0275 (5)
H53A	0.4303	0.5368	0.2599	0.033*
C54	0.41779 (17)	0.47667 (15)	0.35789 (15)	0.0262 (5)
H54A	0.4470	0.5222	0.3972	0.031*
C55	0.38519 (17)	0.40160 (15)	0.38174 (14)	0.0243 (5)
H55A	0.3922	0.3959	0.4375	0.029*
C56	0.34204 (15)	0.33406 (14)	0.32452 (13)	0.0198 (4)
H56A	0.3199	0.2827	0.3414	0.024*
C61	0.34969 (14)	0.26155 (13)	0.10613 (13)	0.0165 (4)
C62	0.32553 (16)	0.30440 (14)	0.03019 (13)	0.0212 (4)
H62A	0.2651	0.3327	0.0033	0.025*

C63	0.39018 (18)	0.30563 (15)	-0.00604 (14)	0.0265 (5)
H63A	0.3741	0.3352	-0.0575	0.032*
C64	0.47799 (18)	0.26375 (15)	0.03285 (15)	0.0270 (5)
H64A	0.5212	0.2636	0.0072	0.032*
C65	0.50297 (16)	0.22220 (15)	0.10861 (15)	0.0246 (5)
H65A	0.5637	0.1946	0.1355	0.030*
C66	0.43901 (15)	0.22086 (14)	0.14555 (14)	0.0199 (4)
H66A	0.4561	0.1922	0.1976	0.024*
Н	0.1541	0.1182	0.1265	0.050*

Table 5. Atomic displacement parameters (\mathring{A}^2)

	U^{11}	U^{22}	U^{33}	U^{12}	U^{13}	U^{23}
Ir	0.01032 (4)	0.01089 (4)	0.01358 (4)	0.00006 (2)	0.00458 (3)	0.00055 (2)
Cl	0.0133 (2)	0.0196 (2)	0.0142 (2)	0.00022 (17)	0.00406 (17)	0.00028 (17)
C1	0.0160 (9)	0.0126 (9)	0.0166 (9)	-0.0001 (7)	0.0055 (8)	0.0009 (7)
O	0.0284 (8)	0.0232 (8)	0.0220 (8)	-0.0003 (6)	0.0133 (7)	-0.0020 (6)
S	0.0164 (2)	0.0173 (2)	0.0219 (2)	0.00096 (18)	0.01092 (19)	-0.00120 (18)
P1	0.0119 (2)	0.0121 (2)	0.0159 (2)	-0.00012 (18)	0.00515 (18)	0.00048 (18)
P2	0.0134 (2)	0.0121 (2)	0.0145 (2)	0.00015 (18)	0.00639 (18)	0.00113 (18)
C2	0.0197 (10)	0.0178 (10)	0.0304 (11)	0.0001 (8)	0.0136 (9)	-0.0032 (9)
C3	0.0295 (12)	0.0256 (12)	0.0359 (13)	0.0031 (9)	0.0222 (11)	0.0010 (10)
C4	0.0303 (13)	0.0299 (13)	0.0522 (16)	-0.0002 (10)	0.0286 (12)	-0.0015 (11)
C5	0.0194 (11)	0.0334 (13)	0.0543 (16)	0.0002 (10)	0.0161 (11)	-0.0050 (12)
C6	0.0193 (11)	0.0248 (11)	0.0392 (13)	0.0022 (9)	0.0096 (10)	0.0004 (10)
C7	0.0216 (11)	0.0256 (11)	0.0311 (12)	0.0003 (9)	0.0124 (9)	0.0019 (9)
C8	0.0205 (13)	0.078 (2)	0.072 (2)	0.0001 (15)	0.0202 (14)	0.0075 (19)
C11	0.0176 (9)	0.0140 (10)	0.0206 (10)	0.0026 (7)	0.0064 (8)	-0.0005 (7)
C12	0.0227 (11)	0.0219 (12)	0.0643 (18)	-0.0042 (10)	0.0185 (12)	-0.0154 (12)

C13	0.0285 (13)	0.0267 (13)	0.079(2)	-0.0075 (11)	0.0217 (14)	-0.0271 (14)
C14	0.0249 (12)	0.0275 (12)	0.0431 (15)	0.0058 (10)	0.0107 (11)	-0.0141 (11)
C15	0.0188 (10)	0.0260 (11)	0.0281 (11)	0.0053 (9)	0.0096 (9)	-0.0007 (9)
C16	0.0178 (10)	0.0166 (10)	0.0226 (10)	0.0015 (8)	0.0073 (8)	0.0010 (8)
C21	0.0220 (10)	0.0109 (9)	0.0171 (9)	-0.0011 (7)	0.0073 (8)	0.0020 (7)
C22	0.0252 (11)	0.0152 (10)	0.0243 (11)	-0.0032 (8)	0.0111 (9)	0.0013 (8)
C23	0.0461 (14)	0.0175 (10)	0.0239 (11)	-0.0046 (10)	0.0201 (11)	-0.0008 (8)
C24	0.0543 (16)	0.0154 (10)	0.0162 (10)	-0.0012 (10)	0.0096 (10)	0.0003 (8)
C25	0.0353 (13)	0.0185 (11)	0.0205 (11)	0.0047 (9)	0.0014 (9)	0.0015 (9)
C26	0.0254 (11)	0.0166 (10)	0.0218 (11)	0.0019 (8)	0.0058 (9)	0.0009 (8)
C31	0.0141 (9)	0.0134 (9)	0.0206 (10)	-0.0011 (7)	0.0083 (8)	-0.0022 (7)
C32	0.0221 (11)	0.0169 (10)	0.0246 (11)	-0.0022 (8)	0.0101 (9)	0.0018 (8)
C33	0.0261 (11)	0.0183 (10)	0.0321 (12)	-0.0069 (9)	0.0175 (10)	-0.0019 (9)
C34	0.0166 (10)	0.0228 (11)	0.0334 (12)	-0.0049 (8)	0.0123 (9)	-0.0078 (9)
C35	0.0175 (10)	0.0242 (11)	0.0221 (10)	-0.0018 (8)	0.0050(8)	-0.0024 (8)
C36	0.0185 (10)	0.0180 (10)	0.0203 (10)	-0.0032 (8)	0.0093 (8)	-0.0021 (8)
C41	0.0165 (9)	0.0149 (9)	0.0195 (10)	0.0014 (7)	0.0074 (8)	0.0055 (7)
C42	0.0219 (10)	0.0219 (10)	0.0198 (10)	-0.0007 (8)	0.0066 (8)	0.0009 (8)
C43	0.0244 (11)	0.0348 (13)	0.0228 (11)	-0.0020 (10)	0.0012 (9)	0.0052 (10)
C44	0.0216 (12)	0.0366 (14)	0.0382 (14)	0.0085 (10)	0.0024 (11)	0.0106 (11)
C45	0.0260 (12)	0.0269 (12)	0.0417 (14)	0.0103 (10)	0.0120 (11)	0.0043 (11)
C46	0.0223 (11)	0.0205 (10)	0.0243 (11)	0.0033 (8)	0.0096 (9)	0.0023 (8)
C51	0.0151 (9)	0.0145 (9)	0.0180 (9)	0.0017 (7)	0.0061 (7)	-0.0009 (7)
C52	0.0319 (12)	0.0152 (10)	0.0235 (11)	-0.0030 (9)	0.0125 (9)	0.0004 (8)
C53	0.0352 (13)	0.0149 (10)	0.0326 (12)	-0.0055 (9)	0.0144 (10)	-0.0015 (9)
C54	0.0294 (12)	0.0173 (10)	0.0276 (11)	-0.0025 (9)	0.0079 (10)	-0.0062 (9)
C55	0.0286 (12)	0.0241 (11)	0.0190 (10)	-0.0018 (9)	0.0089 (9)	-0.0041 (8)
C56	0.0213 (10)	0.0191 (10)	0.0204 (10)	-0.0030 (8)	0.0103 (8)	-0.0010 (8)

C61	0.0194 (9)	0.0133 (9)	0.0194 (10)	-0.0021 (7)	0.0106 (8)	-0.0017 (7)
C62	0.0262 (11)	0.0176 (10)	0.0211 (10)	-0.0015 (8)	0.0112 (9)	-0.0001 (8)
C63	0.0381 (13)	0.0255 (11)	0.0222 (11)	-0.0067 (10)	0.0189 (10)	-0.0011 (9)
C64	0.0338 (12)	0.0244 (11)	0.0337 (12)	-0.0090 (9)	0.0248 (11)	-0.0080 (9)
C65	0.0227 (11)	0.0204 (10)	0.0363 (12)	-0.0030 (8)	0.0179 (10)	-0.0039 (9)
C66	0.0198 (10)	0.0184 (10)	0.0239 (10)	-0.0021 (8)	0.0116 (9)	-0.0005 (8)

Table 6. Geometric parameters (Å, °)

Geometric parameters (Å, °)

Ir—C1	1.880 (2)	C22—C23	1.392 (3)
Ir—P2	2.3611 (5)	C23—C24	1.386 (4)
Ir—P1	2.3757 (5)	C24—C25	1.382 (4)
Ir—S	2.4173 (5)	C25—C26	1.393 (3)
Ir—Cl	2.4933 (5)	C31—C36	1.394 (3)
C1—O	1.136 (2)	C31—C32	1.403 (3)
S—C2	1.792 (2)	C32—C33	1.396 (3)
P1—C21	1.829 (2)	C33—C34	1.387 (3)
P1—C31	1.829 (2)	C34—C35	1.384 (3)
P1—C11	1.833 (2)	C35—C36	1.393 (3)
P2—C41	1.816 (2)	C41—C46	1.397 (3)
P2—C61	1.822 (2)	C41—C42	1.399 (3)
P2—C51	1.833 (2)	C42—C43	1.393 (3)
C2—C7	1.396 (3)	C43—C44	1.384 (4)
C2—C3	1.400 (3)	C44—C45	1.387 (4)
C3—C4	1.384 (4)	C45—C46	1.393 (3)
C4—C5	1.401 (4)	C51—C56	1.393 (3)
C5—C6	1.375 (4)	C51—C52	1.402 (3)
C5—C8	1.510 (4)	C52—C53	1.387 (3)

C6—C7	1.384 (3)	C53—C54	1.389 (3)
C11—C16	1.394 (3)	C54—C55	1.384 (3)
C11—C12	1.395 (3)	C55—C56	1.398 (3)
C12—C13	1.396 (3)	C61—C62	1.395 (3)
C13—C14	1.384 (4)	C61—C66	1.397 (3)
C14—C15	1.384 (3)	C62—C63	1.392 (3)
C15—C16	1.390 (3)	C63—C64	1.386 (4)
C21—C26	1.396 (3)	C64—C65	1.382 (3)
C21—C22	1.401 (3)	C65—C66	1.392 (3)
C1—Ir—P2	90.90 (6)	C15—C16—C11	120.6 (2)
C1—Ir—P1	94.28 (6)	C26—C21—C22	119.21 (19)
P2—Ir—P1	174.495 (17)	C26—C21—P1	119.81 (16)
C1—Ir—S	171.87 (6)	C22—C21—P1	120.74 (16)
P2—Ir—S	89.315 (17)	C23—C22—C21	120.4 (2)
P1—Ir—S	85.292 (17)	C24—C23—C22	119.8 (2)
C1—Ir—Cl	94.52 (6)	C25—C24—C23	120.3 (2)
P2—Ir—Cl	90.580 (16)	C24—C25—C26	120.4 (2)
P1—Ir—Cl	90.857 (16)	C25—C26—C21	119.9 (2)
S—Ir—Cl	93.603 (17)	C36—C31—C32	118.71 (19)
O—C1—Ir	174.67 (18)	C36—C31—P1	119.55 (15)
C2—S—Ir	109.21 (7)	C32—C31—P1	121.74 (16)
C21—P1—C31	105.52 (9)	C33—C32—C31	120.1 (2)
C21—P1—C11	104.31 (9)	C34—C33—C32	120.4 (2)
C31—P1—C11	104.47 (9)	C35—C34—C33	119.8 (2)
C21—P1—Ir	112.59 (6)	C34—C35—C36	120.1 (2)
C31—P1—Ir	114.92 (7)	C35—C36—C31	120.8 (2)
C11—P1—Ir	114.01 (7)	C46—C41—C42	119.40 (19)
C41—P2—C61	106.31 (9)	C46—C41—P2	121.24 (16)

C41—P2—C51	103.21 (9)	C42—C41—P2	118.94 (16)
C61—P2—C51	101.32 (9)	C43—C42—C41	120.1 (2)
C41—P2—Ir	111.42 (7)	C44—C43—C42	120.1 (2)
C61—P2—Ir	111.12 (7)	C43—C44—C45	120.3 (2)
C51—P2—Ir	122.01 (7)	C44—C45—C46	120.1 (2)
C7—C2—C3	117.4 (2)	C45—C46—C41	120.1 (2)
C7—C2—S	124.15 (17)	C56—C51—C52	119.15 (19)
C3—C2—S	118.18 (18)	C56—C51—P2	123.39 (16)
C4—C3—C2	121.4 (2)	C52—C51—P2	117.45 (16)
C3—C4—C5	121.1 (2)	C53—C52—C51	120.7 (2)
C6—C5—C4	116.9 (2)	C52—C53—C54	119.8 (2)
C6—C5—C8	121.3 (3)	C55—C54—C53	119.9 (2)
C4—C5—C8	121.8 (3)	C54—C55—C56	120.6 (2)
C5—C6—C7	123.0 (2)	C51—C56—C55	119.7 (2)
C6—C7—C2	120.3 (2)	C62—C61—C66	119.64 (19)
C16—C11—C12	118.8 (2)	C62—C61—P2	124.08 (16)
C16—C11—P1	120.13 (15)	C66—C61—P2	116.21 (15)
C12—C11—P1	121.08 (17)	C63—C62—C61	119.8 (2)
C11—C12—C13	120.2 (2)	C64—C63—C62	120.1 (2)
C14—C13—C12	120.5 (2)	C65—C64—C63	120.4 (2)
C13—C14—C15	119.5 (2)	C64—C65—C66	119.9 (2)
C14—C15—C16	120.4 (2)	C65—C66—C61	120.1 (2)

Compound IV from Chapter Four

Table 7. Fractional atomic coordinates and isotropic or equivalent isotropic displacement parameters (\mathring{A}^2)

	x	y	z	$U_{ m iso}$ */ $U_{ m eq}$
C1	0.0000	1.0000	-0.2876 (10)	0.0175 (9)
S1	-0.03539 (6)	0.91979 (3)	-0.06282 (18)	0.01471 (17)
S2	0.24846 (7)	0.93745 (3)	0.02398 (19)	0.01883 (18)
C2	0.1175 (3)	0.88829 (14)	0.0443 (7)	0.0131 (5)
C3	0.1164 (3)	0.81355 (15)	0.1613 (7)	0.0123 (5)
C4	0.0165 (3)	0.76672 (14)	0.0741 (7)	0.0139 (5)
H4A	-0.0525	0.7832	-0.0581	0.017*
C5	0.0182 (3)	0.69657 (15)	0.1803 (7)	0.0157 (6)
H5A	-0.0498	0.6654	0.1185	0.019*
C6	0.1171 (3)	0.67090 (15)	0.3750 (7)	0.0155 (6)
C7	0.2168 (3)	0.71736 (14)	0.4594 (8)	0.0158 (6)
H7A	0.2858	0.7006	0.5908	0.019*
C8	0.2167 (3)	0.78758 (15)	0.3547 (7)	0.0147 (6)
H8A	0.2855	0.8183	0.4149	0.018*
C9	0.1180 (3)	0.59434 (15)	0.4914 (8)	0.0230 (7)
H9A	0.0416	0.5696	0.4081	0.035*
Н9В	0.1171	0.5934	0.7295	0.035*
Н9С	0.1960	0.5704	0.4120	0.035*

Table 8. Atomic displacement parameters (Å²)

	U^{11}	U^{22}	U^{33}	U^{12}	U^{13}	U^{23}
C1	0.030(2)	0.0082 (17)	0.0141 (19)	0.0029 (16)	0.000	0.000
S 1	0.0150(3)	0.0111 (3)	0.0180(3)	0.0020(2)	-0.0025 (3)	0.0006 (3)

S2	0.0145 (3)	0.0119 (3)	0.0300 (4)	-0.0012 (2)	0.0034(3)	0.0004 (3)
C2	0.0145 (12)	0.0125 (12)	0.0123 (12)	0.0012 (9)	0.0007 (12)	-0.0025 (11)
C3	0.0127 (12)	0.0113 (12)	0.0129 (13)	0.0014 (11)	0.0023 (10)	-0.0016 (11)
C4	0.0122 (12)	0.0143 (12)	0.0153 (13)	0.0011 (10)	0.0007 (12)	-0.0017 (11)
C5	0.0155 (13)	0.0133 (13)	0.0181 (13)	-0.0017 (11)	0.0027 (11)	-0.0033 (11)
C6	0.0191 (14)	0.0118 (13)	0.0154 (15)	0.0032 (10)	0.0065 (11)	-0.0005 (11)
C7	0.0161 (13)	0.0169 (12)	0.0144 (13)	0.0044 (10)	0.0000 (11)	0.0023 (11)
C8	0.0149 (13)	0.0131 (12)	0.0160 (14)	0.0009 (10)	0.0006 (10)	-0.0018 (10)
C9	0.0316 (16)	0.0128 (12)	0.0247 (19)	0.0030 (11)	0.0052 (14)	0.0024 (13)

Table 9. Geometric parameters (Å, °)

Geometric parameters (Å, °)

•					
C1—S1 ⁱ	1.804 (2)	C3—C4	1.404 (4)		
C1—S1	1.804 (2)	C4—C5	1.386 (4)		
S1—C2	1.747 (3)	C5—C6	1.388 (4)		
S2—C2	1.643 (3)	C6—C7	1.395 (4)		
C2—C3	1.482 (4)	C6—C9	1.514 (4)		
C3—C8	1.397 (4)	C7—C8	1.386 (4)		
S1 ⁱ —C1—S1	118.3 (2)	C5—C4—C3	120.2 (3)		
C2—S1—C1	103.12 (10)	C4—C5—C6	121.4 (3)		
C3—C2—S2	123.6 (2)	C5—C6—C7	118.3 (3)		
C3—C2—S1	113.26 (19)	C5—C6—C9	121.1 (3)		
S2—C2—S1	123.13 (16)	C7—C6—C9	120.6 (3)		
C8—C3—C4	118.4 (3)	C8—C7—C6	121.1 (3)		
C8—C3—C2	120.6 (3)	C7—C8—C3	120.6 (3)		
C4—C3—C2	120.9 (2)				
Symmetry code: (i) $-x$, $-y+2$, z .					

For all compounds all e.s.d.'s (except the e.s.d. in the dihedral angle between two l.s. planes) are estimated using the full covariance matrix. The cell e.s.d.'s are taken into account individually in the estimation of e.s.d.'s in distances, angles and torsion angles; correlations between e.s.d.'s in cell parameters are only used when they are defined by crystal symmetry. An approximate (isotropic) treatment of cell e.s.d.'s is used for estimating e.s.d.'s involving l.s. planes.